

Resilience assessment of water distribution networks under pipe failures based on a hydraulically-informed graph approach

AUTHOR

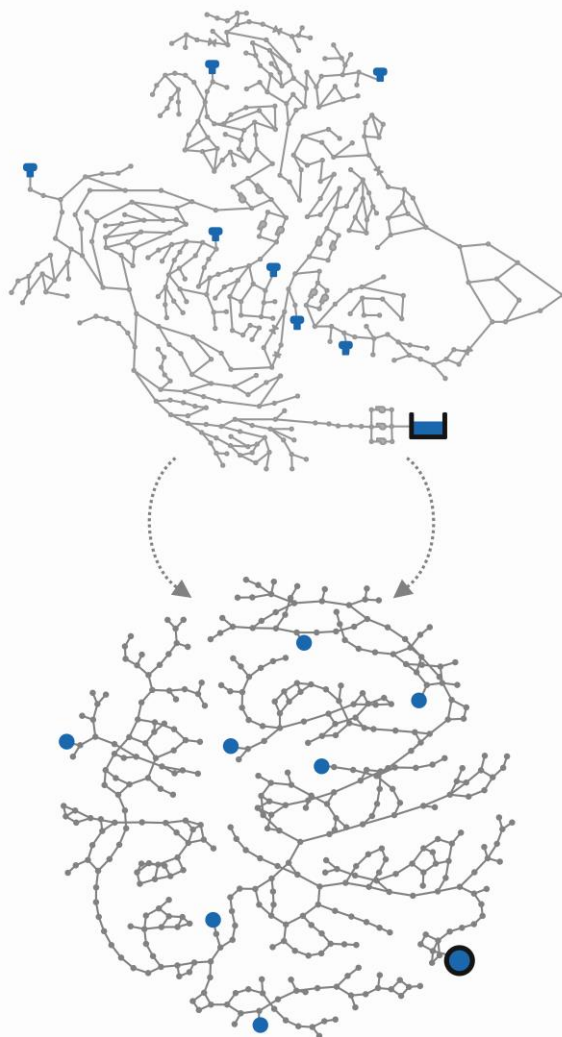
Mohsen Hajibabaei

SUPERVISORS

Prof. Robert Sitzenfrei
Prof. Mohsen Shahandashti
Prof. Michelle Hummel
Prof. Oswald Jenewein

PUBLISHER

Austrian Marshall Plan Foundation
Vienna, Austria



Resilience assessment of water distribution networks under pipe failures based on a hydraulically-informed graph approach

Author: Mohsen Hajibabaei¹

Supervisors: Prof. Robert Sitzenfrei¹, Prof. Seyed Mohsen Shahandashti², Prof. Michelle A Hummel², Prof. Oswald Jenewein³

¹Unit of Environmental Engineering, Department of Infrastructure Engineering, University of Innsbruck, Innsbruck, Austria.

²Department of Civil Engineering, University of Texas at Arlington, Arlington, Texas, USA.

³School of Architecture, University of Texas at Arlington, Arlington, Texas, USA

Contents

- 1. Introduction-----4**
- 1. 1 Background -----4**
- 1. 2 Problem statement -----5**
- 1. 3 Aim of the study -----6**
- 2. Materials & methods -----6**
- 2.1. Resilience analysis based on hydraulic simulations -----6**
- 2.1.1 Single pipe failures----- 7
- 2.1.2 Multiple pipe failures under earthquake ----- 9
- 2.1.2.1 Integrated Multi-physics modeling and Monte Carlo simulation -----11
- 2.2. Resilience analysis based on graph theory----- 12**
- 2.2.1 Graph representation of WDNs -----12
- 2.2.2 Background of Graph metrics for WDNs-----12
- 2.2.3 HGA for resilient assessment under pipe failures -----15
- 2.2.3.1 Identifying critical pipes for single-source WDNs -----15
- 2.2.3.2 Identifying critical pipes for multi-source WDNs -----20
- 3. Case studies ----- 21**
- 4. First results ----- 22**
- 4.1 Single pipe failures for the first case study ----- 22**
- 4.2 Single pipe failures for the second case study ----- 26**
- 4.3 Multiple pipe failures for the third case study ----- 27**
- 5. Next steps ----- 28**
- 6. Appendix----- 29**
- 7. References----- 33**

1. Introduction

Water distribution networks (WDNs) as pivotal urban infrastructures are responsible for delivering water with adequate quality and quantity to the public. They face various spectrums of disruptive events that threaten their functionality. These events are categorized into natural disasters (e.g., earthquakes, hurricanes, floods) and human-made disasters (e.g., overloading, terrorist attacks, cyber-attacks) (Assad, Moselhi, and Zayed 2019; Diao et al. 2016). Water infrastructures are made of multiple elements which interact in a complex way (Sitzenfrei et al. 2020). Therefore, due to their high level of complexity, minor disturbances can trigger cascading events causing crucial impacts on the well-being and safety of residents (Shuang, Zhang, and Yuan 2014; Zhang et al. 2020). Supplementary to these, the aging of networks increases their vulnerability, which causes an increase in the likelihood of interruption in their functionality during and after disasters (Diao et al. 2016). Consequently, these infrastructures need to be robust enough to cope with any disruption with the least impact on their functionality. This is where resilience is emerging as a significant consideration in the planning of WDNs (Assad et al. 2019). Resilience can be defined as the ability of networks to maintain and adapt their operational performance over design life, in the face of adverse conditions (Herrera, Abraham, and Stoianov 2016; Strigini 2012).

Various definitions have been documented to quantify the concept of resilience in WDNs (Herrera et al. 2016). Common approaches use hydraulic models and formulate resilience as a measure (e.g., the ability of a system to maintain water supply under adverse conditions). These approaches are known as performance-based or hydraulic-based, requiring hydraulic simulations during multiple failure scenarios (Pagano et al. 2019). A primary drawback of hydraulic-based approaches is that the analysis may become very computationally intensive, specifically when it comes to large-scale networks (Herrera et al. 2016). In addition, detailed input information regarding hydraulic models is required to do such analyses. Another mathematical tool for quantifying the resilience of WDNs is graph-based approaches, which are less computationally intensive and data-dependent compared to hydraulic models (Pagano et al. 2019). Graph-based approaches analyze WDNs from the topological perspectives, mainly focusing on connectivity, diversity, and redundancy as structural properties (Butler et al. 2017). In these approaches, a WDN is presented as a graph with nodes (e.g., reservoirs and tanks) interconnecting via edges (e.g., pipes, valves, and pumps). This paper focuses on the application of graph-based approaches for the resilience assessment of WDNs.

1. 1 Background

Over the past few years, new graph-based approaches have been introduced in the literature for several tasks of WDNs modeling (Giustolisi, Ridolfi, and Simone 2019; Herrera et al. 2016; Lorenz, Altherr, and Pelz 2021; Sitzenfrei et al. 2021). Giustolisi et al., (2019) customized certain graph metrics according to WDNs characterization to predict the hydraulic behavior of these networks. Simone et al. (2020) applied one of those customized metrics (i.e., edge betweenness) to seven WDNs to underline the role of topological attributes in water flow prediction. Sitzenfrei et al. (2020) introduced a customized metric for distributing water flow in networks and developed a highly efficient approach for the Pareto-optimal design of WDNs. In addition, graph-based approaches have been successfully applied for water quality assessment (Sitzenfrei 2021), efficient water quality sensor placement (Giudicianni et al. 2020), and identification of network patterns in optimal WDNs (Sitzenfrei, Oberascher, and Zischg 2019).

Several studies have been conducted on the resilience assessment of WDNs using graph-based approaches (Pagano et al. 2019; Yazdani, Dueñas-Osorio, and Li 2013). Employing various graph metrics provides simplified and general information on resilience. Average node degree, link density, meshedness coefficient, and average path length are all instances of these graph metrics (Hwang and Lansey 2017; Torres et al. 2017; Yazdani et al. 2013; Yazdani, Otoo, and Jeffrey 2011). Such metrics have been widely used in literature as surrogate indicators for the resilience evaluation of WDNs (Pandit and Crittenden 2016; Perelman et al. 2015; Yazdani et al. 2011; Zhao, Chen, and Gong 2015). However, the inherent constraint of these metrics is that they cannot properly reflect the hydraulic behavior of networks as they only focus on the topological and structural attributes. Meng et al., (2018) showed that although topology could have a significant impact on the performance of WDNs, not all the topological graph metrics are suitable as surrogate resilience indicators.

To account for the hydraulic behavior of WDNs, Herrera et al. (2016) suggested using topological constants (i.e., pipe length and pipe diameter) as a potential surrogate measure for energy loss corresponding with water transport routes in a network. Since Herrera's approach relies only on the topological attributes, Lorenz et al. (2019) modified this approach by considering pipe resistance as a physical feature of water routes. Pagano *et al.*, (2019) highlighted the potentials and limitations of graph-based approaches compared to a hydraulic-based method for resilience assessment of WDNs. Their results showed that the graph-based approaches could have high reliability to identify critical pipes for networks with simple structures. They also introduced a particular graph measure based on network connectivity to evaluate the impact of single pipe failures on the resilience of WDNs. This measure only relies on the topological features such as the length and diameter of pipes and overlooks the role of water flow on the resilience assessment. Chen, Vladeanu, and Daly (2021) used two standard graph metrics (i.e., betweenness centrality and bridge metric) to quantify pipe criticality in WDNs. Their idea was to present a graph technique as a potential surrogate for hydraulic simulations. However, they could not find any correlation between the graph metrics and the hydraulic behavior of pipes. The reason is that the metrics applied in their study cannot evaluate the capacity and redundancy of pipes. Moreover, the effects of nodal demand and water flow were neglected from their analysis.

1. 2 Problem statement

The aforementioned graph-based approaches applied for the resilience assessment of WDNs are mostly dependent on topological and structural perspectives and independent of the impacts of hydraulic characteristics (e.g., water flow and pipe capacity). Since hydraulic variables affect friction losses and nodal pressure (Rossman 2000), neglecting their impacts could considerably influence the accuracy of resilience analysis. Another drawback of conventional graph approaches is that they cannot investigate the consequences of failures on the other components of WDNs. In other words, failure propagation and, therefore, the 'local response' of networks to failure modes is not clear in their resilience analysis. In addition, the proposed graph-based methods are incapable of considering the impact of multiple failures on resilience. They also need to be tailored to consider the characteristics of WDNs with multiple sources. These research gaps need to be addressed by developing a graph theory-based approach that can consider the effects of the hydraulic behavior of WDNs under various failure modes.

1. 3 Aim of the study

This paper aims to propose a hydraulically-informed graph-based approach (HGA) to assess the resilience of WDNs due to pipe failures. In this context, HGA is a modification to the regular graph applications of WDNs, wherein the graph weighting functions are proportionally derived from the hydraulic and structural characteristics to mimic the hydraulic behavior. Using this approach, specific graph measures are introduced to identify critical pipes and better understand the 'local response' of WDNs under different failure modes (i.e., single and multiple pipe failures). The topological and hydraulic features of WDNs, such as pipes capacity, network connectivity, and the impact of nodal demand, are considered in this method. Besides, this research explores to what extent the suggested HGA can be used as a hydraulic surrogate for the resilience enhancement of WDNs in case of multiple pipe failures due to earthquakes.

2. Materials & methods

This study investigates the effects of different failure modes on the resilience of WDNs. These modes include single pipe failures, firefighting (excess demand on nodes), multiple pipe failures due to earthquakes, and a combination of multiple and simultaneous failures. Currently, we just focus on single and multiple pipe failures, but this study will be extended, and other modes will be added to it in the future. The suggested resilience evaluation procedure is as follows:

- 1) First, based on a hydraulic model simulation, the level of failure magnitude resulting from single pipe failures is assessed, and critical pipes are ranked. For multiple pipe failures, earthquake scenarios are created using earthquake modeling, and the failure magnitude of each scenario is calculated based on the hydraulic simulations. These scenarios are then ranked according to their magnitude.
- 2) Second, conventional graph metrics used in literature for resilience analysis are introduced. Thereafter, we propose an HGA to investigate the impacts of pipe failures on resilience and identify critical pipes (for single pipes failures) and critical scenarios (for multiple pipe failures).
- 3) Third, the pipe and scenario rankings obtained from (1) are then compared with those derived from HGA in step (2).
- 4) Forth, after successfully validating the results in (3), an HGA framework is proposed for the resilience enhancement of WDNs in case of multiple pipe failures that occurred due to earthquakes.
- 5) Fifth, the accuracy of the proposed framework in (4) is evaluated by comparing the results with a simulated annealing-based optimization approach which is integrated with a network-level seismic assessment model.

It is worth mentioning that due to the high computational burdens of the optimization approach in the (5), the fourth and fifth steps will be added to this study in the future. Besides, this research will be extended by conducting a comprehensive literature review on the seismic rehabilitation of WDNs.

2.1. Resilience analysis based on hydraulic simulations

Hydraulic simulations are executed using the EPANET-MATLAB toolkit (Rossman et al. 2020) based on two different analyses, i.e., demand-driven analysis (DDA) and pressure-driven analysis (PDA). In DDA analysis, nodal demands are always fulfilled regardless of nodal pressure, while PDA assumes demands are satisfied proportional to nodal pressure (Tanyimboh and Templeman

2010). DDA simulations have been traditionally used for the hydraulic modeling of WDNs. However, they may yield unrealistic results, especially under certain circumstances like pipe failure, as providing desired demands is not always possible in such conditions (Gorev et al. 2021; Mahmoud, Savić, and Kapelan 2017).

The hydraulic resilience is evaluated based on two terms: a) serviceability and b) robustness. Serviceability is the ability of a system to maintain water supply under adverse conditions, and it is a common approach to formulate hydraulic resilience (Herrera et al. 2016). Any disruption in WDNs could lead to the loss of serviceability which results in supply failure. Robustness can be defined as the ability of the system to reduce the impacts of failures (Jung, Lee, and Kim 2019). Therefore, the more robust a WDN is, the less is the magnitude of 'supply failure'. In this study, we defined resilience as a level to which a WDN minimizes supply failure and robustness failure magnitude in the face of adverse conditions. The procedure of resilience assessment of WDNs under single and multiple pipe failure is described in the following.

2.1.1 Single pipe failures

The framework of resilience assessment based on the hydraulic model is shown in Fig. 1. In this framework, single pipe failures are modeled by adjusting the status of pipes to 'closed' for 24 h in EPANET. To account for demand changes over one day, a standard demand pattern with 24-hourly multipliers is defined (see Fig. 2). In this figure, the demand multiplier of the peak demand (Q_{design}) is 1.0 and the average demand (Q_{avg}) over one day is $Q_{\text{avg}} = 0.62 Q_{\text{design}}$.

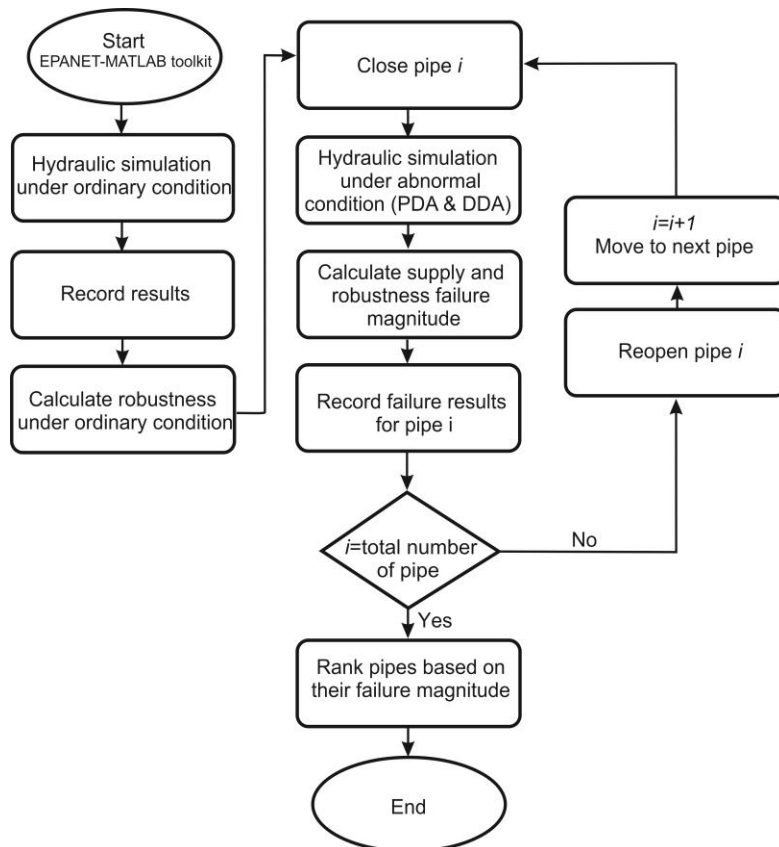


Fig. 1. Flowchart of the calculation steps for the hydraulic model

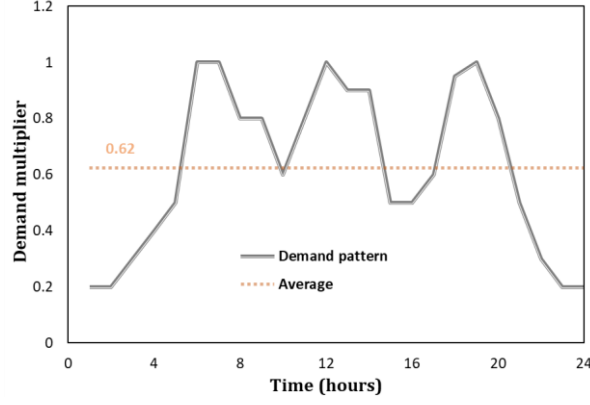


Fig. 2. Diurnal demand pattern

Two indicators, i.e., a) supply failure magnitude and b) robustness failure magnitude, are applied as measures to identify critical pipes and evaluate the resilience of WDNs.

The supply failure magnitude resulting from pipe failure over one day is calculated as follows:

$$\text{Supply failure magnitude} = \frac{\sum_0^{t=T} (\sum_0^{i=n} (D_{i,t} - S_{i,t}))}{\sum_0^{t=T} (\sum_0^{i=n} D_{i,t})} \quad (1)$$

Where, $D_{i,t}$ is the required demand of node i at time t (l/s), $S_{i,t}$ is the supplied demand (i.e., outflow) of node i at time t (l/s), T is the time steps (h), and n is the number of nodes.

The supplied demand is calculate using EPANET 2.2 which can implement both PDA and DDA approaches (Rossman et al. 2020). In this software, Wagner's equation (Wagner, Shamir, and Marks 1988) is applied, and the supplied demand (outflow) of each node at each time step is calculated as follows:

$$\text{if } P_{i,t} \leq P_{min} : S_{i,t} = 0$$

$$\text{if } P_{min} < P_{i,t} < P_{req} : S_{i,t} = D_{i,t} \cdot \left(\frac{P_{i,t} - P_{min}}{P_{req} - P_{min}} \right)^\gamma \quad (2)$$

$$\text{if } P_{i,t} \geq P_{req} : S_{i,t} = D_{i,t}$$

Where $P_{i,t}$ is the pressure of node i at time t , P_{min} is the minimum pressure (i.e., pressure below which the outflow is zero), P_{req} is the required pressure to deliver full demand, and γ is the pressure exponent. In this paper, P_{min} and P_{req} are considered 0 and 30 m, respectively (ÖNORM 2018), and γ is set equal to 0.5 (Gorev et al. 2021).

The robustness failure magnitude is estimated using Eq. 3, which represents pressure failure resulting from pipe failures compared to the ordinary condition.

$$\text{Robustness failure magnitude} = 1 - \frac{Rob_{abnormal}}{Rob_{normal}} \quad (3)$$

$Rob_{abnormal}$ and Rob_{normal} are robustness under abnormal (i.e., single pipe failures) and normal (i.e., ordinary) conditions, respectively, where robustness itself is calculated as follows:

$$Rob = \frac{\sum_0^{t=T} (\sum_0^{i=n} (D_{i,t} \cdot PI_{i,t}))}{\sum_0^{t=T} (\sum_0^{i=n} D_{i,t})} \quad (4)$$

Where, $D_{i,t}$ is the required demand of node i at time t (l/s), n is the number of nodes, and $PI_{i,t}$ is the 'performance index' of node i at time t which is calculated based on the penalty curve shown in Fig. 3 (Hajibabaei, Nazif, and Sitzenfreni 2019; Tabesh and Zia 2003).

According to this Figure, the value of 1 describes the excellent performance level, and 0.75, 0.5, and 0.25 show suitable, acceptable, and unsuitable levels, respectively. H_{des} is the desired nodal pressure recommended by standard codes (ÖNORM 2018), satisfying demand and enough water pressure for consumers. The desired (H_{des}) and maximum (H_{max}) pressures in Fig. 3 are set to 60 m and 100 m, respectively. H_1 , H_2 , and H_3 are the pressures in which outflow is equal to 0.25, 0.5, and 0.75 of required nodal demand, respectively, calculated based on H_{des} as follows (Tabesh and Zia 2003):

$$H_1 = \frac{1}{16}H_{des}, H_2 = \frac{1}{4}H_{des}, H_3 = \frac{9}{16}H_{des} \quad (5)$$

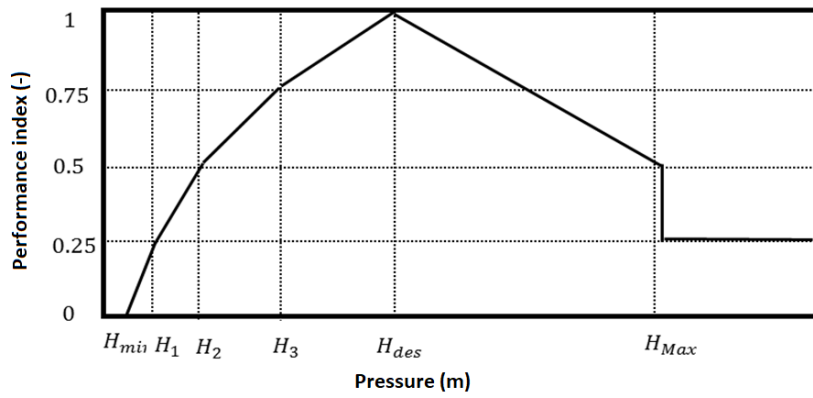


Fig. 3. Penalty curve of nodal pressure for calculating performance index (PI) of each node at each time step.

After performing hydraulic simulation under single pipe failure mode, critical pipes are identified and ranked regarding their level of failure magnitude.

2.1.2 Multiple pipe failures under earthquake

In order to create the earthquake scenarios, the first step is to calculate the seismic repair rate (repairs per 1000 ft. of pipe) for each pipe. Fig. 4 illustrates the required steps to calculate the seismic repair rate for each pipe. We need to identify the earthquake with the highest contribution (i.e., highest value) in the initial stage, known as scenario earthquake. The scenario earthquake is chosen based on deaggregation analysis. USGS (2018) is used to conduct the deaggregation analysis considering the spatial relationship among seismic intensities (Adachi 2007; Jayaram and Baker 2009; Weatherill et al. 2013; Zanini et al. 2016; Zanini, Faleschini, and Pellegrino 2017).

After the selection of the scenario earthquake, peak ground velocity (PGV) is calculated using the ground motion prediction equation (GMPE) (Abrahamson and Silva 2007; Zanini et al. 2016, 2017). The general equation is given by the following equation:

$$\log_{10}(PGV_{mn}) = f(M_m, R_{mn}, \theta_m) + \delta_x v_m + \delta_y \epsilon_{mn} \quad (6)$$

Where PGV_{mn} = value of peak ground velocity at location n from source m ; R_{mn} = distance between location m and location n ; M_m = earthquake magnitude; θ_m = fault geological parameters at location m ; $\delta_x v_m$ = the interevent residual; and $\delta_y \epsilon_{mn}$ = the intra-event residual. Scenario shake map

calculator is used to create a peak ground velocity map (Field et al. 2005). The value of ε_{mn} is estimated using Eq. 7 (Weatherill et al. 2013; Zanini et al. 2016).

$$\varepsilon = M + V.L \quad (7)$$

Where M = Mean value of normally distributed v_m and ε_{mn} ; L = Lower triangular matrix; V = vector of random variables with normal distribution. The value of M is considered as 0. Cholesky decomposition method was applied to find the value of L , such that $LL^T = CoV$. CoV is the covariance matrix, which can be calculated based on the following equation.

$$CoV = \begin{bmatrix} 1 & \delta(d_{1,2}) & \dots & \delta(d_{1,N}) \\ \vdots & 1 & \dots & \delta(d_{2,N}) \\ \vdots & \vdots & \ddots & \vdots \\ sym & \vdots & \dots & 1 \end{bmatrix} \quad (8)$$

Where $\delta(d_{m,n})$ is a correlation coefficient between intra-event residuals for location m and location n . The value of $\delta(d_{m,n})$ can be estimated using Eq. 9 (Jayaram and Baker 2009).

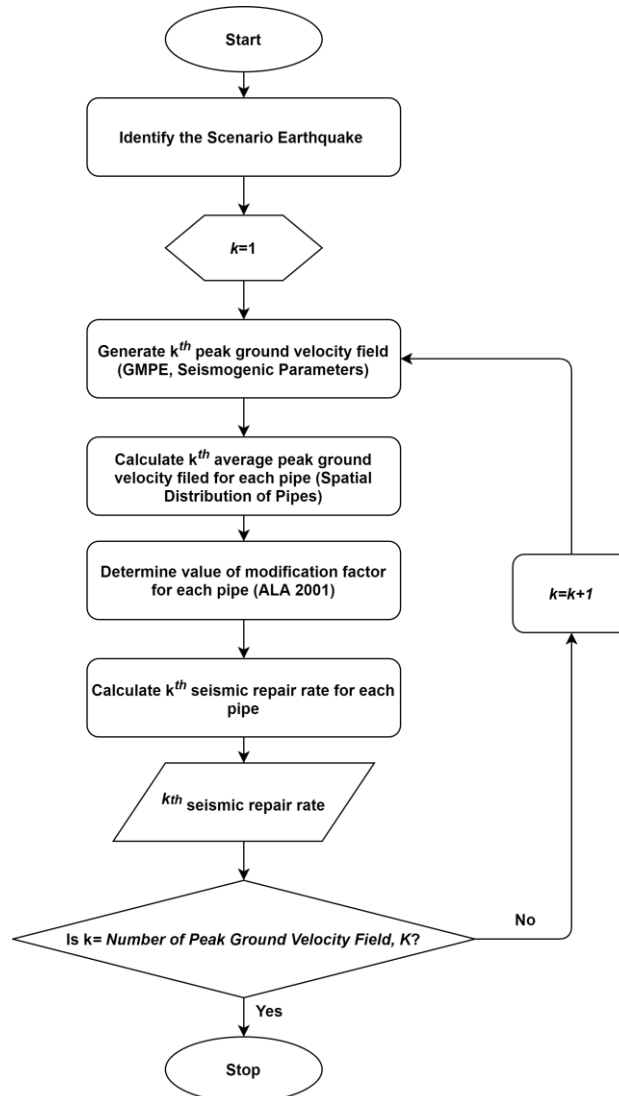


Fig. 4. Steps of calculating seismic repair rate of each pipe

$$\delta(d_{m,n}) = e^{\left(\frac{-d_{m,n}}{r}\right)} \quad (9)$$

Where $d_{m,n}$ = distance between location m and location n ; and r is the intersite distance. According to (Wang and Takada 2005), the value of r can be considered between 20 km - 40 km. The whole thing is repeated for K times to create K random PGV fields (Zanini et al. 2017). Seismic pipe repair rates for each pipe are then determined based on ALA (2001):

$$RR_{i,k} = Mod * 0.00187 * PGV_{i,k} \quad (10)$$

$RR_{i,k}$ is this equation the seismic pipe repair rate per 1000 ft of pipe i for the k th seismic PGV field. Mod is the modification factor that adjusts the value of the repair rate considering the corrosivity of soil, pipe diameter, pipe material, and pipe joint characteristics.

2.1.2.1 Integrated Multi-physics modeling and Monte Carlo simulation

Supply failure magnitude in case of an earthquake is calculated using Eq.1 and Monte Carlo simulation. The procedure is indicated in Fig. 5.

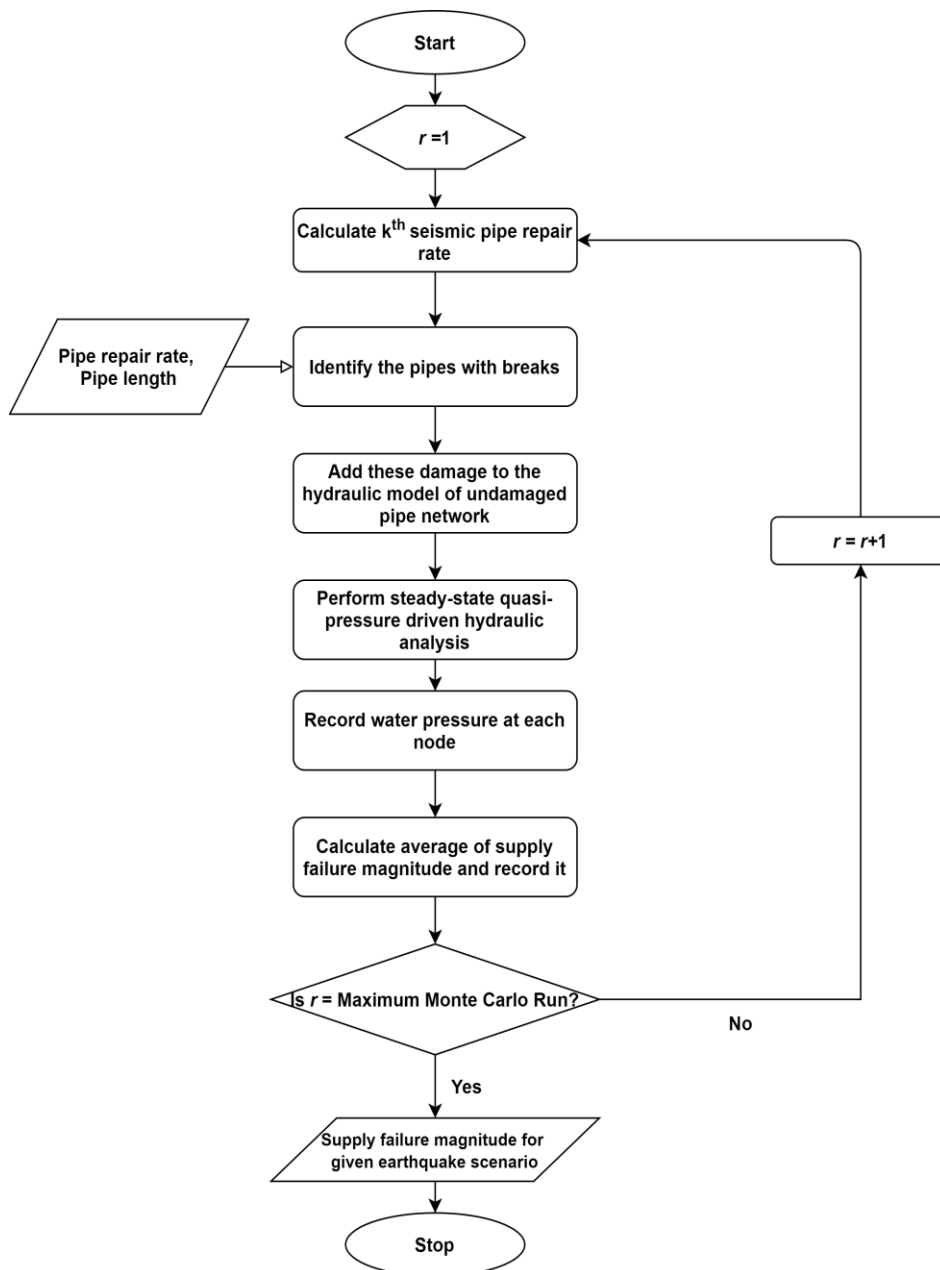


Fig.5. Steps of Monte Carlo simulation for a given earthquake scenario for the k th PGV field

Only breaks are considered in this study as seismic damage. After determining if there is a break in the pipe or not, the breaks are combined into the hydraulic model of the original network, and pressure at each node is determined.

For every Monte Carlo simulation, the following steps are:

- 1) Analyzing the network, including breaks
- 2) Removing nodes having negative pressure
- 3) Step 1 and step 2 are repeated if there is any node with negative pressure.

Afterward, the supply failure magnitude for the predefined maximum Monte Carlo runs is calculated using Eq. 11:

$$Supply\ failure\ magnitude_{avg} = \frac{1}{K} \cdot \sum_{k=1}^K Supply\ failure\ magnitude_k \quad (11)$$

Where $Supply\ failure\ magnitude_k$ is the value of failure magnitude calculated based on Eq. 1; and K is the total number of PGV fields. In the end, the value of supply failure magnitude for each Monte Carlo run is then recorded.

2.2. Resilience analysis based on graph theory

2.2.1 Graph representation of WDNs

Urban water networks can be described with a specific branch of mathematics known as graph theory. Accordingly, WDNs can be modeled as a mathematical graph G composed of $\#N$ (vertices/nodes) connected by a set of $\#E$ (edges/pipes). The structural connection between nodes of graph G is expressed by elements a_{ij} of an adjacency matrix A ($\#N \times \#N$). The element a_{ij} is either 1 or 0. The value of 1 implies a link connecting nodes i and j , and when there is no connection, the value is 0. Graph G can be weighted or unweighted. All weights of edges/nodes in an unweighted graph are equal to 1. In a weighted graph, different weights can be assigned to each edge k . For instance, structural parameters such as pipe length (L_k) and pipe diameters (DN_k), or (simulated) hydraulic parameters such as water flow (Q_k) and friction loss (h_k), or their combinations (e.g., $L_k \cdot Q_k / DN_k$) can be used as weighting functions. With the aid of these weighted graphs of water networks, various graph investigations can be conducted. As an example, the weights representing travel time (e.g., L_k/DN_k) can be used as surrogate measures for water age or water quality-related analysis (Sitzenfrei et al. 2019).

2.2.2 Background of Graph metrics for WDNs

This section describes some conventional metrics and certain modified measures, which provide general information regarding the resilience analysis of WDNs. In literature, the following metrics have been suggested.

The degree of a node is the number of edges (e.g., pipes) connected to it. It can also be averaged throughout the entire system, referred to as **average node degree** (ND_{avg}) (Newman 2010). Higher values of ND_{avg} indicate multiple paths, which can be interpreted as higher redundancy (Hwang and Lansey 2017). The corresponding equation is given by Eq. 12:

$$ND_{avg} = \frac{2 \cdot \#E}{\#N} \quad (12)$$

Where, $\#E$ is the number of edges, and $\#N$ is the number of nodes.

Further, the **meshedness coefficient** (R_m) (Buhl et al. 2006) expresses the fraction between the actual number of independent loops in a network and the maximum number of loops (Eq. 13). The range of R_m is between 0 (tree-like networks) and 1 (grid-like networks), implying that the larger the values of R_m , the more connected the WDN (Pagano et al. 2019).

$$R_m = \frac{\#E - \#N + 1}{2\#N - 5} \quad (13)$$

The **density of bridge** (D_{br}) in a WDN represents the ratio of edges whose failure isolate a part of a network (i.e., bridges) to the total number of edges, which is calculated based on the following equation (Yazdani et al. 2011):

$$D_{br} = \frac{\#E_{br}}{\#E} \quad (14)$$

Where, $\#E_{br}$ is the number of bridges and $\#E$ is the number of edges.

Shortest path length (SPL) is another metric utilized in the literature for several tasks of WDNs modeling. SPL between two nodes i and j describes the shortest distance between these nodes. In this context, distance refers to the sum of all edge weights in the path that connects these two nodes (Dijkstra 1959). Depending on modeling tasks, various kinds of weights can be assigned to edges for SPL calculation. For instance, pipe length divided by pipe diameter (L_k/DN_k) was used by Herrera et al. (2016) as a weighting function for SPL to consider friction losses along pipes.

Edge betweenness centrality (EBC) has been used in literature to indicate the significance of edges in a WDN. $EBC(k)$ is the EBC of the edge k , which measures how often k is a part of the SPL from a source s (e.g., tank) to every node $i \in N$ (Brandes 2008):

$$EBC(k) = \sum_{s,i \in N} SPL_{s,i}(k) \quad (15)$$

For example, Fig. 6a shows that when we calculate the SPL from every node to the source node with an unweighted graph, the edge between $N1$ and $N2$ is only once part of the shortest path. In contrast, the connected edge to the source occurs seven times in SPL ($EBC(k) \in [0, \#N]$).

Sitzenfrei et al. (2020) added a modification to the EBC , specifically for WDNs analysis, referred to as **demand edge betweenness centrality** (EBC^Q). As illustrated in Fig. 6b, EBC^Q determines the SPL connecting the source node s and every demand node i , and adds the demands of node i ($Q_i > 0$) to the corresponding path. The $EBC^Q(k) \in [0, \sum_{s,i \in N} Q_i]$ is calculated as follows:

$$EBC^Q(k) = \sum_{s,i \in N} SPL_{s,i}(k) \cdot Q_i \quad (16)$$

The EBC^Q indicated in Fig. 6b was calculated using the weighting function of pipe length and can be used for the optimal design of WDNs (Sitzenfrei et al. 2020). The weights applied for this example are static. However, Sitzenfrei et al. (2020) introduced a new term for weighting graphs, denoted 'dynamic weights', where the edges' weights can be changed iteratively. In this study, we add a customized modification to the proposed 'dynamic weights' (described in section 2.2.3) and apply it for the resilience analysis of WDNs.

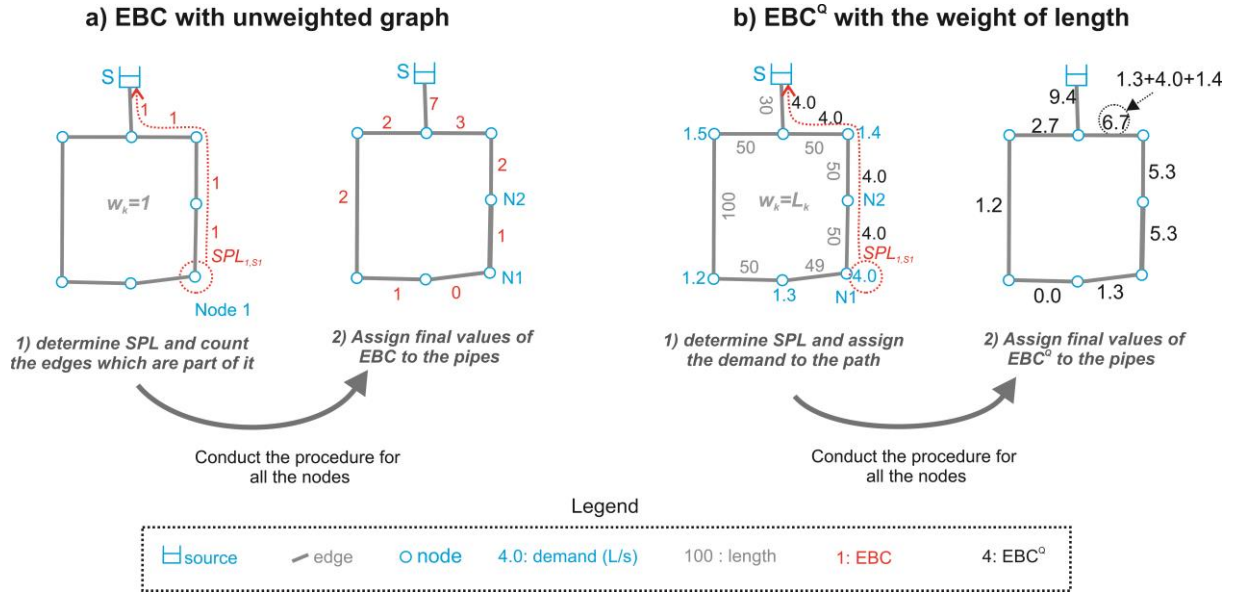


Fig. 6. Calculating EBC and EBC^Q for a simplified WDN.

Local graph theory measures for pipe ranking (LGTM) is an approach including topological metrics to identify crucial pipes in WDNs under single pipe failures, which was proposed by Pagano et al. (2019). LGTM is conducted based on the comparison between $SPL_{s,i,0}$ (the SPL from each water source to all other nodes under normal conditions), with the SPL resulting from the removal of edge m , i.e., $SPL_{s,i,m}$. Accordingly, three potential scenarios are possible for removing an edge $m \in E$ from a WDN (Pagano et al. 2019).

- If there are no changes in the $SPL_{s,i,m}$ compared to the $SPL_{s,i,0}$, the impact of the edge failure on the resilience of WDNs is neglectable.
- If the $SPL_{s,i,m}$ returns infinity, it can be interpreted as a disconnection between a node(s) and sources. Therefore, the impact of the edge failure ($D(m)$ in Eq. 17) is estimated by calculating the total nodal demand ($\sum_{j \in N} Q_j$) that becomes isolated from all water sources as follows:

$$D(m) = \sum_{s=1}^S \sum_{j \in N} Q_j \quad (17)$$

Edges with a high value of $D(m)$ are then ranked accordingly to highlight the critical pipes.

- If the $SPL_{s,i,m}$ increases compared to $SPL_{s,i,0}$, the consequence of the edge failure on the resilience of WDNs is estimated by the SPL changes ($SPLC_{s,i,m} = SPL_{s,i,m} - SPL_{s,i,0}$) as follows:

$$SPLC(m) = \sum_{s=1}^S \sum_{i \in N} SPLC_{s,i,m} \quad (18)$$

Edges with a high value of $SPLC(m)$ are ranked and considered as critical pipes.

LGTM creates two subsets of pipes (edges) based on $D(m)$ and $SPLC(m)$, and pipes with higher values in each subset are considered as the critical elements. In this paper, we compare the results of our proposed HGA with LGTM to underline the potentials and limitations of both approaches.

2.2.3 HGA for resilient assessment under pipe failures

Resilient operation of WDNs depends on network connectivity (i.e., the existence of redundant paths between nodes), as well as hydraulic heads and energy losses (Ulusoy, Stoianov, and Chazerain 2018). Using this concept, an HGA is proposed to evaluate the resilience of WDNs without conducting any hydraulic simulations. The proposed approach is based on the EBC^Q (Eq. 16) introduced by Sitzenfrei et al. (2020) for the design of WDNs. However, a modification is added to it herein, denoted *dynamic* EBC^Q (EBC_D^Q), which can mimic the hydraulic characteristics of existing WDNs by applying proper dynamic weights. The framework of the proposed HGA is elucidated using simple examples in the following sections.

2.2.3.1 Identifying critical pipes for single-source WDNs

In this section, EBC_D^Q calculation for a single-source WDN is first explained and then applied for critical pipes identification.

The procedure of calculating EBC_D^Q is similar to EBC^Q , and the only difference is in applying the weighting function. When it comes to determining SPL and EBC^Q for existing WDNs, we usually access information such as pipe diameter and roughness, which can be applied as graph weights. However, an appropriate weighting function is required to be derived from the hydraulic and structural characteristics to mimic the hydraulics of pipes.

In order to fulfill the water supply in a WDN, a flow at a source needs to find its optimal pathway to its demand node. We know from the hydraulic behavior of WDNs that water flow tends to choose the path with the least hydraulic resistance. Accordingly, pipe resistance can be integrated into the weighting function of SPL to explain this event. The hydraulic resistance of an edge k can be estimated using Eq. 19 (Lorenz and Pelz 2020).

$$r_k \approx f_k \cdot \frac{L_k}{D_k} \quad (19)$$

Where, L_k is the length of edge k , D_k is the diameter of edge k , and f_k is the pipe's friction factor calculated as follows, assuming the turbulent flow in pipes (Lorenz et al. 2021):

$$f_k = (2 \log_{10} (D_k/a_k) + 1.74)^{-2} \quad (20)$$

Where, a_k is the roughness of edge k .

Once a path with the minimum resistance from the water source to a node is found, the corresponding demand (water flow) is routed from the source to the demand node. That causes an additional friction loss (resistance) along that path. Consequently, to fulfill the energy balance in the WDN, the next flow package from the source to the demand node may avoid taking the path used before by the previous flow package. This issue can be addressed by applying the dynamic weight for EBC^Q (i.e., EBC_D^Q), which modifies the weights (Eq. 19) iteratively. Fig. 7 shows a simplified example for EBC_D^Q calculation.

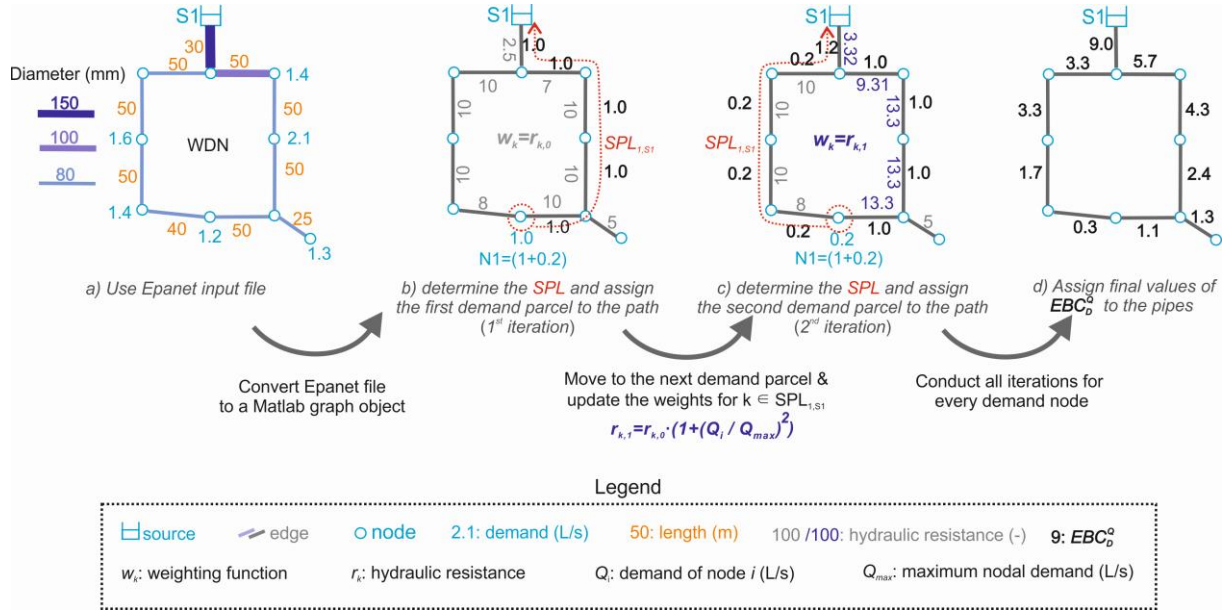


Fig. 7. Applying dynamic weights to calculate dynamic demand edge betweenness centrality (EBC_D^Q)

According to this figure, the Epanet input file of WDN is first converted to the MATLAB graph objective (Fig. 7a). Then the hydraulic resistance of pipes is calculated using Eq. 19, and the values are assigned to the pipes as weights (gray-colored numbers). Additionally, the demand for each node is divided into packages to mimic flow package routing in real WDNs. The procedure is initiated by the node with the minimum non-zero demand value (i.e., N1). As shown in Fig. 7b, $SPL_{1,S1}$ is the path between node 1 and source 1 where the hydraulic resistance of pipes is minimal. After determining $SPL_{1,S1}$, the first demand parcel of node 1 (i.e., 1 l/s) is added to the corresponding path (red-colored route) to calculate EBC_D^Q . Routing the first parcel from N1 to the source causes additional resistance in the corresponding path. Therefore, the hydraulic resistance of the flow path in the first iteration is artificially lengthened by the factor of $1 + (Q_1/Q_{max})^2$, where Q_{max} is the maximum nodal demand in the networks. This lengthening factor allows the next demand parcel in the second iteration to be routed through the alternative path to the left branch (Fig. 7c). This procedure is repeated for all the demand nodes and final values of EBC_D^Q are calculated by summing up the EBC_D^Q of pipes obtained in each iteration (Fig. 7d).

The proposed approach described in Fig. 7, takes into account the resistance of pipes, demands of nodes, and alternative supply paths between sources and demand nodes, without performing any hydraulic simulations. Also, the principal idea of the lengthening factor (i.e., $1 + (Q_i/Q_{max})^2$) is derived from the Darcy-Weisbach equation where friction loss/resistance is proportional to Q^2 (Hajibabaei, Hesarkazzazi, and Sitzenfrei 2021). This lengthening factor indicates that small demands in a WDN are usually routed through the shortest paths with the least resistance. In contrast, large demands tend to travel through more alternative paths, which are not necessarily the shortest path. This idea is in agreement with the concept of energy balance in WDNs.

After calculating EBC_D^Q , we create a failure matrix F ($\#E \times \#E$) for the pipe ranking under single pipe failures. The element f_{mn} in F shows the failure consequence of the edge (pipe) n on the edge m and is determined as follows:

First, according to the procedure illustrated in Fig. 7, EBC_D^Q is calculated under normal conditions and based on the average nodal demand using the following dynamic weight:

$$r_{k,j} = r_{k,j-1} \cdot (1 + (Q_i/Q_{max})^2) \quad (21)$$

Where, $r_{k,j-1}$ is the hydraulic resistance of each k-shortest path between node i and source s in the j^{th} iteration (m/m), Q_i is the demand of node i (L/s), and Q_{max} is the maximum nodal demand that exists in the network (L/s).

Second, an edge $n \in E$ is removed from the graph of WDN (see Fig. 8), which is considered as the pipe failure. In this situation, two scenarios are possible:

- (1) After the edge failure, no path exists between the nodes connecting the edge n , and therefore, at least one node becomes disconnected from the source (see Fig. 8b). This means removing the edge leads to cutting off part of the network which cannot be supplied anymore. In this case, the total demand that is not fulfilled is equal to the EBC_D^Q routed through the failed edge in the normal condition. Therefore, we allocate the $EBC_D^Q(n)_{normal}$ to $f_{n,n}$ as the failure effect of the edge n (see Fig. 8b), and assign zero to the other elements (i.e., $f_{m,n}=0, m \neq n$).

$$f_{n,n} = EBC_D^Q(n)_{normal} \quad (22)$$

Where, $EBC_D^Q(n)_{normal}$ is the dynamic demand edge betweenness centrality of the edge n (L/s) under the ordinary condition. As shown in Fig. 8d, nonzero values on the main diagonal of the failure matrix F are related to the pipes whose failure isolates a part of the WDN from the source (i.e., $p1$ and $p5$).

- (2) In the second scenario, the edge failure does not isolate part of the network but changes the connectivity between the source and the demand nodes. In this case, the failure consequence is assessed by investigating its impacts on the other edges (pipes). For instance, when the edge $P2$ ($n = p2$) fails (Fig. 8c), the load on it (i.e., EBC_D^Q) is borne by the other edges. These edges can be identified by comparing their $EBC_D^Q(m)_{abnormal}$ with $EBC_D^Q(m)_{normal}$. Fig. 8c indicates that the load on the edge $P2$ is redistributed through the orange-colored pipes with the $\Delta EBC_D^Q(m)_{p2} = EBC_D^Q(m)_{abnormal,p2} - EBC_D^Q(m)_{normal} > 0$. In the next step, the extra loads on the paths ($\Delta EBC_D^Q(m) > 0$) are compared with the optimal capacity of the edges. As shown in Fig. 8c, the failure effects of edge 2 on the pipes whose excess loads are less than their optimal capacity are neglectable (i.e., $f_{m,2}=0, m=1:6$). On the other hand, the excess loads of the red-colored edges are greater than their optimal capacity. Under those circumstances, the failure consequence of the edge n on the edge m is estimated as follows:

$$f_{m,n} = \frac{\Delta EBC_D^Q(m)_n - C_{opt}(m)}{\delta(m)} \quad (23)$$

Where, $\Delta EBC_D^Q(m)_n$ is the changes of $EBC_D^Q(m)$ due to the failure of the edge n (L/s), $C_{opt}(m)$ is the optimal capacity of the edge m (L/s), and $\delta(m)$ is the overload coefficient of the edge m (-).

$C_{opt}(m)$ is calculated based on the optimal flow velocity $V_{opt}(m)$ of the edge (recommended by the standard codes in Table. 1), and the edge diameter $D(m)$ as follows:

$$C_{opt}(m) = V_{opt}(m) \cdot \pi D(m)^2 / 4 \quad (24)$$

Besides, $\delta(m)$ describes the maximum capacity of the edge m regarding its optimal capacity (C_{max}/C_{opt}), and is calculated using Eq. 25.

$$\delta(m) = V_{max} / V_{opt}(m) \quad (25)$$

Where, V_{max} is the maximum acceptable velocity in WDNs (m/s). In this study, 3 m/s is considered for V_{max} (ÖNORM 2018), and V_{opt} values are determined using Table 1.

Table 1: Suggested values for the optimal velocity in WDNs (ÖNORM 2018)

D (mm)	80	100	125	150	200	250	300	350	400	500	600	700
V_{opt} (m/s)	0,80	0,80	0,80	0,85	0,90	0,95	1,00	1,05	1,10	1,20	1,30	1,40
C_{opt} (l/s)	4,0	6,3	9,8	15,0	28,3	46,6	70,7	101	138	236	368	539

This procedure is conducted by removing every edge n ($n = 1:E$) and calculating its impacts on the WDN using Eq. 26. Thereafter, the maximum value of $I(n)$ is determined (*i. e.*, I_{max}), and the graph index (GI) of the failure of edge n is calculated based on Eq. 27.

$$I(n) = \sum_{m=1}^E f_{m,n} \quad (26)$$

$$GI(n) = \frac{I(n)}{I_{max}} \quad (27)$$

Edges with the positive value of $GI(n)$ are identified and ranked accordingly, and particular attention is given to those with the highest values.

For the multiple pipe failures, the failure matrix F consists of $\#E \times \#S$, where S is the number of failure scenarios. The element $f_{m,s}$ in F shows the consequence of the scenario s on the edge m . Similar to single pipe failures (Fig. 8c), if multiple edge failures in scenario s only change the connection of flow path between the source and nodes, the effects of the scenarios are estimated using Eq.26 and 27 (where, $n=s$). However, there could be a scenario like in Fig. 9 (for the same WDN), in which not only a part of the network gets disconnected, but also the connection between the source and the demand nodes is changed. To calculate the element of $f_{m,s}$ in this point, the isolated nodal demand(s) is assigned to the edges whose failure disconnected part of the network from the source (see Fig. 9b). Afterward, the effects of scenario s on the other edges are estimated by identifying the overloaded edges (Fig. 9c) and applying Eq.26 and 27 (where, $n=s$).

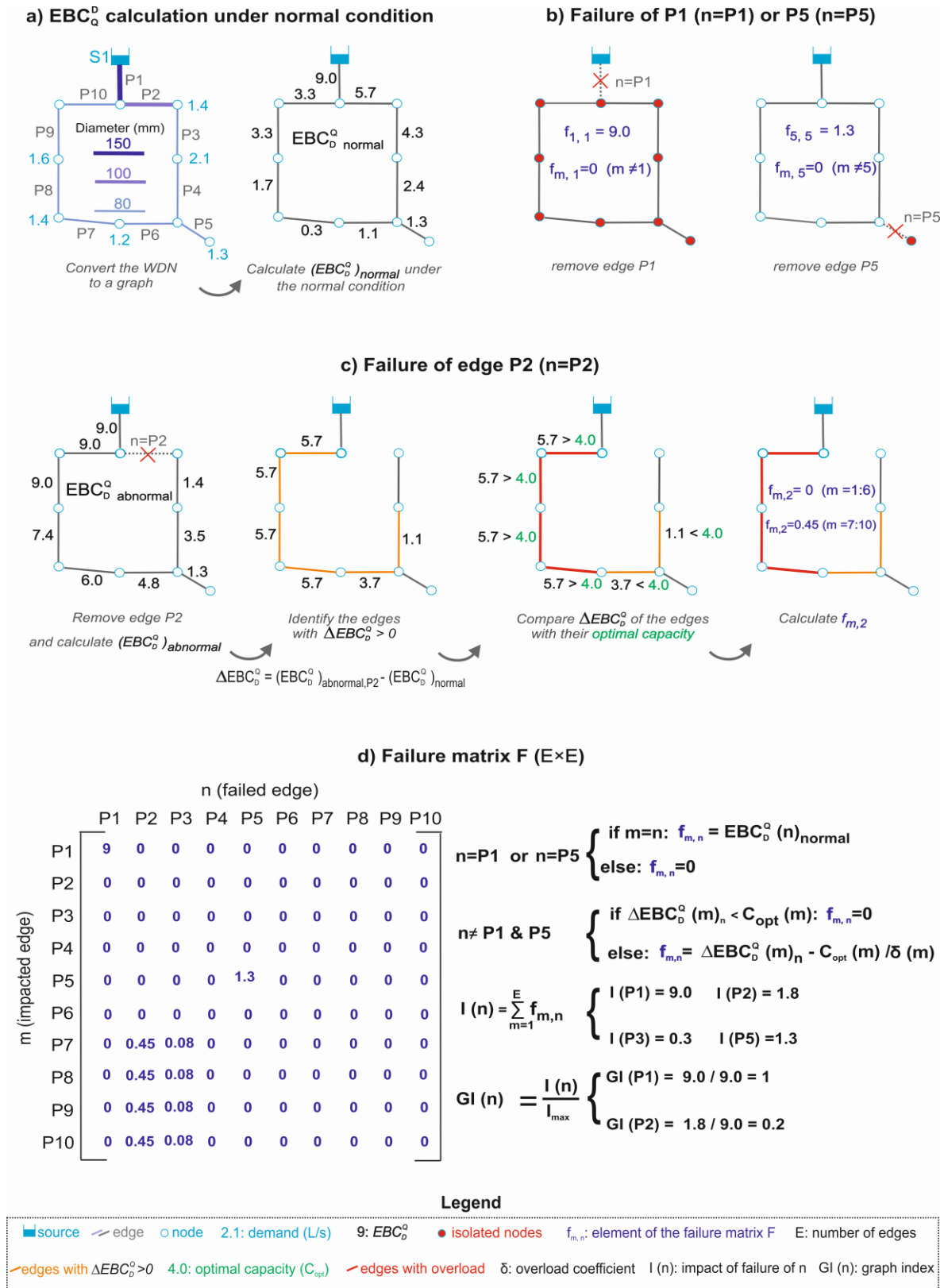


Fig. 8. Pipe ranking under single pipe failures

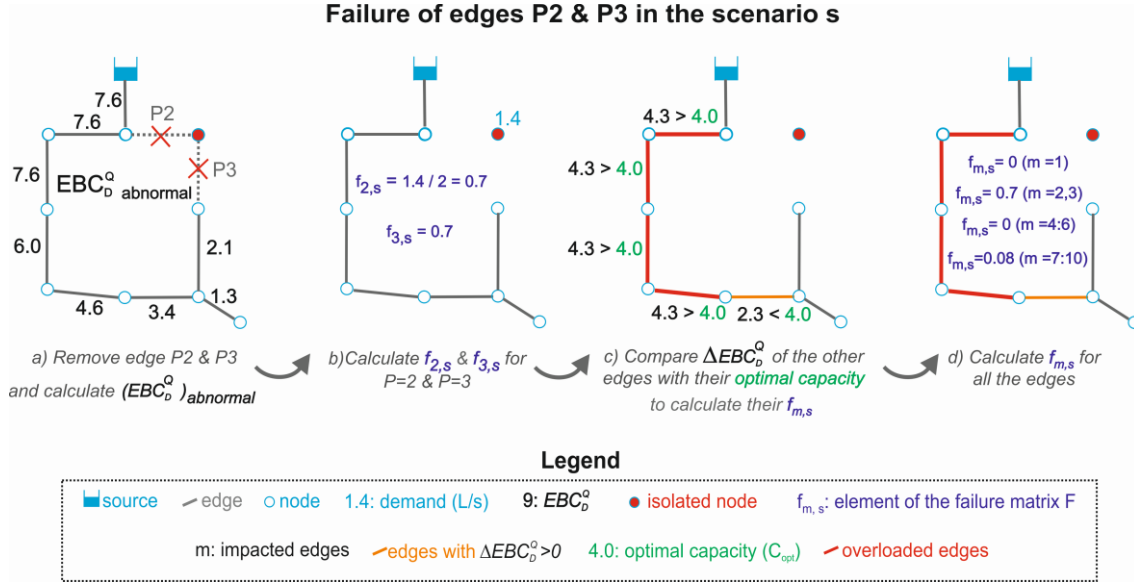


Fig. 9. Multiple edge failure in the scenario s

2.2.3.2 Identifying critical pipes for multi-source WDNs

The effect of single pipe failures on multi-source WDNs is investigated in this section. For this purpose, the first step is to conduct the source tracing for every node. As shown in Fig. 10, the nodes in the multi-source WDN are supplied by the sources based on their nodal heads. The nodal head i is estimated by subtracting the energy (head) loss $hf_{i,s}$ along the flow path from the source S with the head H_S (i.e., $H_{i,S} = H_S - hf_{i,s}$). Head losses in hydraulic models can be determined using the Darcy-Weisbach equation (Rossman et al. 2020). Accordingly, energy loss hf_m in each pipe m with the diameter D_m , the length L_m , the friction factor f_m , and the water flow Q_m is calculated as follows (in the SI units):

$$hf_m = \frac{f_m L_m}{12.1 D_m^5} \cdot Q_m^2 \quad (m) \quad (28)$$

f_m is dependent on the flow regime in pipes, which is determined with the Reynolds number (Rossman et al. 2020). Note that the goal here is to simplify the head loss formula in order to use it as a weighting function for the graph-based model without conducting hydraulic simulations. To do so, if we use the expression of $Q_m = v_m \cdot D_m^2 \cdot \pi/4$ in E.q 28, and assume a constant flow velocity (v_m) in all pipes, the following term is derived for the weighting function of w_{static} :

$$w_{static} = c \cdot \frac{L_m}{D_m} \quad (m) \quad (29)$$

Where c with the unit of meter can be interpreted as a hydraulic gradient multiplied by average pipe diameter in WDNs. For instance, hydraulic gradient (friction slope) for optimal WDNs can be assumed to be 20 m/km (i.e., 1/50 m/m) (Sitzenfrei et al. 2020); which means if the average pipe diameter in a network is 0.1 m, the coefficient c is estimated with 1/50.

w_{static} in Eq. 29 can be integrated into the weighting function of SPL to estimate the head loss along the flow path (i.e., $hf_{i,s} \approx SPL_{i,s}$). For this purpose, firstly, the $SPL_{i,s}$ is calculated from the node i to every source S with the static weight of w_{static} . In the second step, the $SPL_{i,s}$ is subtracted from the corresponding source head ($H_{i,s} = H_S - SPL_{i,s}$). Finally, the nodal head ($H_{i,s}$) resulted from

each source are compared, and node i is assigned to the source with a higher value of $H_{i,S}$ (see Fig. 10a). Note that this procedure only presents a simplified assumption to conduct the source tracing, and calculated $H_{i,S}$ with the $SPL_{i,S}$ cannot represent the accurate nodal head.

After conducting the source tracing based on the SPL (Fig 10a), the WDN is divided into two parts in Fig. 10b. The $EBC_D^Q(m)_{normal}$ of each part is calculated based on the dynamic weights similar to single-source WDNs. After an edge failure, the source tracing needs to be repeated because as shown in Fig. 10c, the supplied nodes by each source could be changed due to the failure. Thereafter $EBC_D^Q(m)_{abnormal}$ of each part is determined, and edges are ranked similar to the procedure described for single-source WDNs.

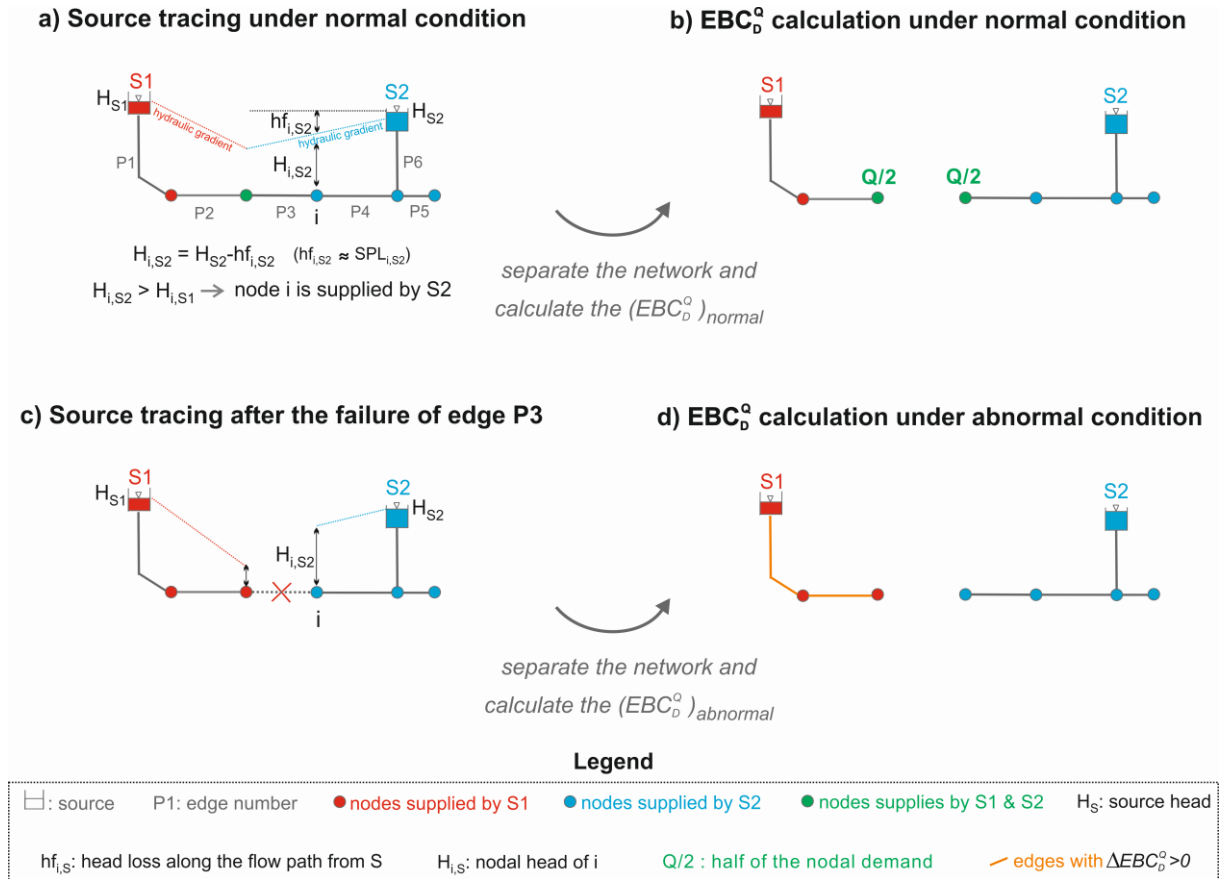


Fig. 10. Source tracing and EBC_D^Q calculation in a multi-source WDN

3. Case studies

Different WDNs are analyzed as case studies to compare the results of the proposed HGA with those obtained from hydraulic simulations. The first case study is a real WDN consisting of 242 junctions, 268 pipes, and a single reservoir. This network was also optimally designed to investigate the effects of different configurations on resilience. The diameters of the optimally designed networks were determined based on the evolutionary algorithm and using the state-of-the-art methodology GALAXY (Wang, Savić, and Kapelan 2017). More information regarding the design procedure can be found in (Sitzenfrei et al. 2020). The second case study (D-Town) is a benchmark WDN with a complex hydraulic behavior comprising 399 junctions, 433 pipes, 11 pumps, 5 valves, 7 storage tanks, and a single reservoir. For this network, the results of HGA under single pipe failures are compared with hydraulic simulations and graph measures suggested in the literature. The third case study (BAK) is also a benchmark network selected to investigate the

impacts of multiple pipe failures (under earthquake scenarios) on resilience. This WDN has 58 pipes, 35 junctions, and a single reservoir.

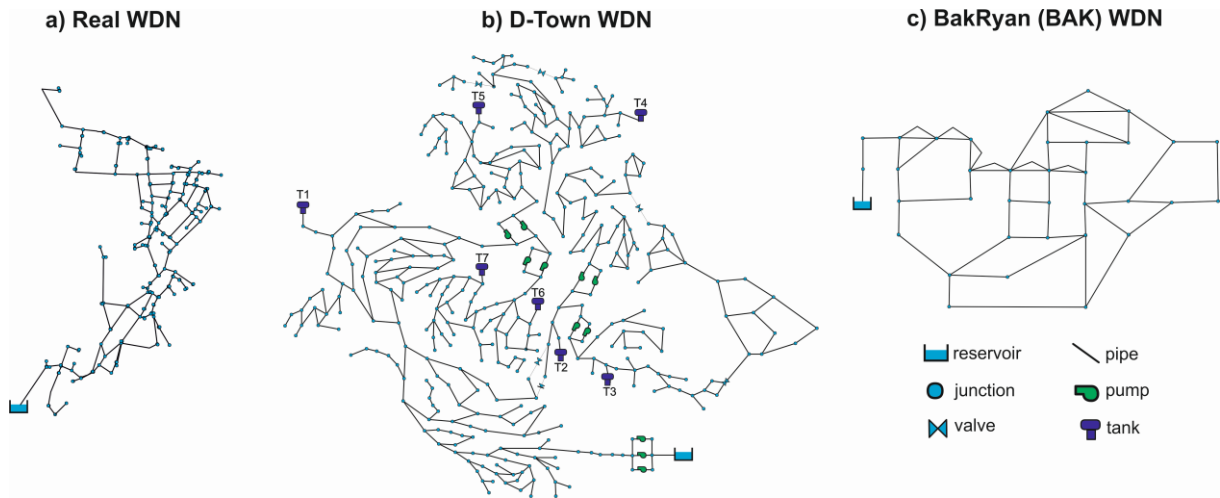


Fig. 11. Layouts of the case studies

The properties of the networks are also indicated in Table 2.

Table 2: Properties of the case studies

	#N	#E	ND_{avg}	R_m	D_{br}	total length (km)	average length (m)
Existing WDN	242	268	2.21	0.05	0.47	14.5	54
D-Town	407	459	2.25	0.07	0.41	61	141
BAK	36	58	3.22	0.34	0.05	25	424

4. First results

4.1 Single pipe failures for the first case study

The impact of network configuration on resilience is assessed by analyzing different networks. For this purpose, the existing network was redesigned for two single-source (Fig. 12b and 12c), and one multi-source WDNs (Fig. 12d). For each network, the critical pipes in terms of supply failure and robustness failure derived from the hydraulic model are compared with those obtained from the proposed HGA.

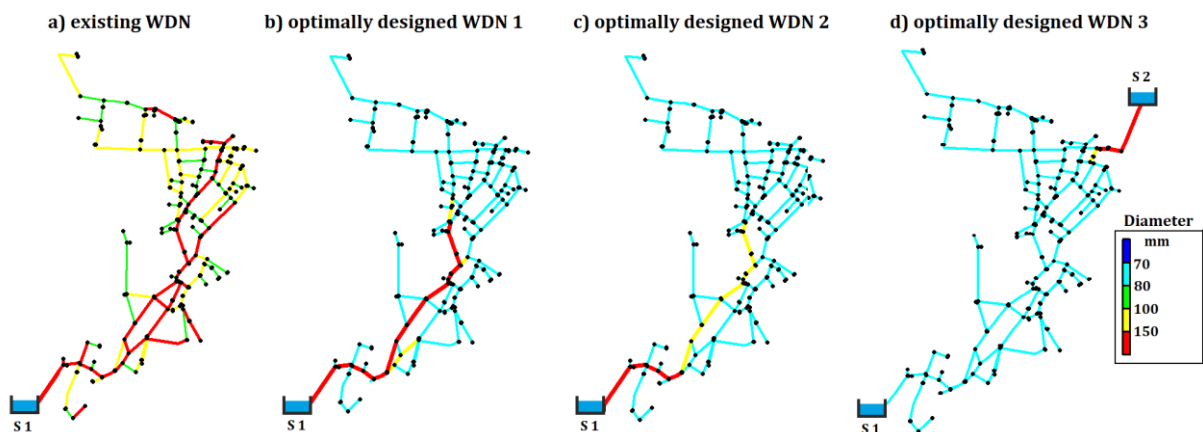


Fig. 12. Considered WDNs for the first case study

Conducting the hydraulic simulations for the existing network (Fig 12a) shows that only 6 pipes (out of 268) impact more than 6% on the supply and robustness indices if they fail individually. The top 6 pipes are all identified by the proposed HGA. As shown in Fig. 13, those are the main pipes whose failure disconnects a major portion of the network. Note that Fig. 13b is the graph drawing of the first case study with force-directed placement, which uniformizes the edge lengths and helps to compare the critical edges better. The existing network is comprised of pipes with enough capacity. Therefore, the failure of a single pipe located in a loop would be compensated by others, highlighting that redundancy plays a crucial role in the resilience of WDNs. We have addressed this issue in HGA by considering alternative supply paths between sources and demand nodes, as well as the capacity of those alternative paths. The critical pipes indices of the existing network obtained from the hydraulic model are indicated in Table A1 in the appendix.

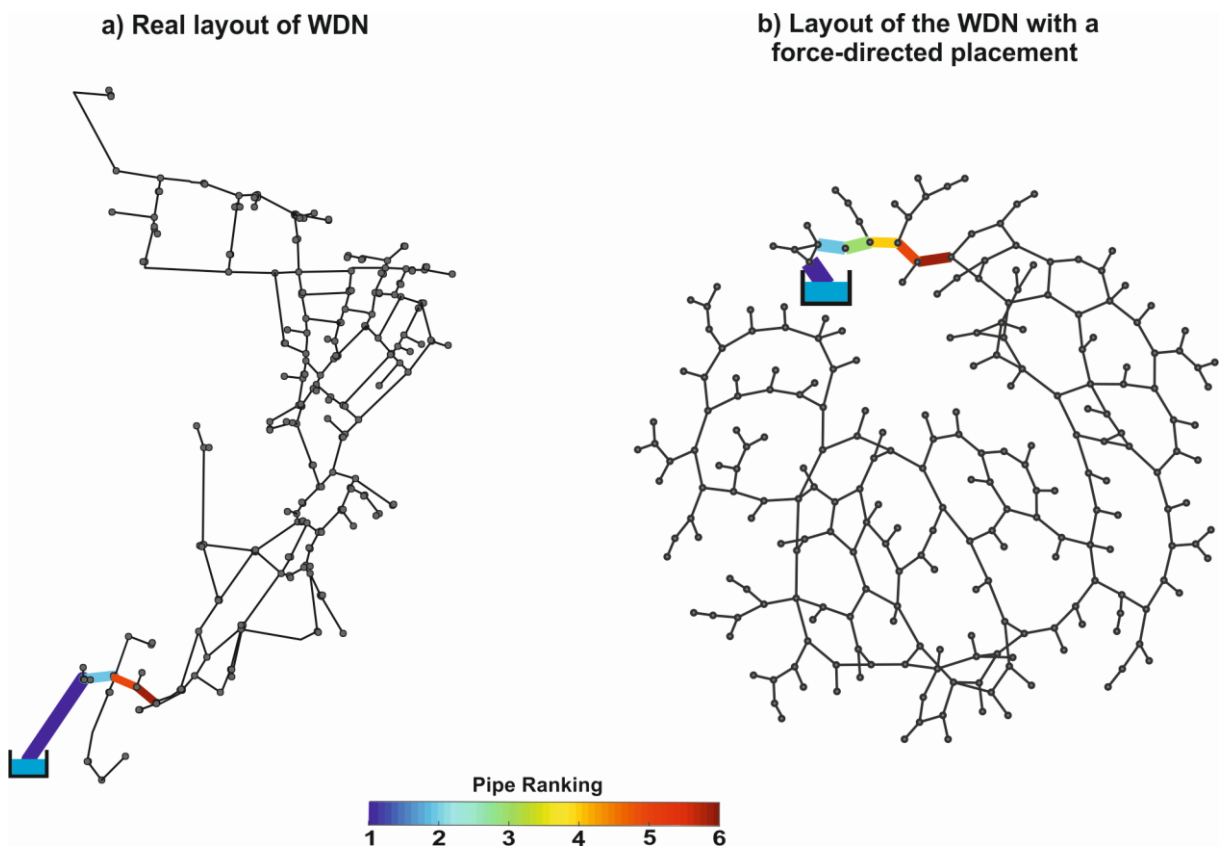


Fig. 13. Critical pipes for the existing WDN with the supply and robustness failure magnitudes of more than 6% under single pipe failures

The resilience analysis of optimally designed WDN 1 indicates that this network is less resilient than the existing WDN. The response of WDN 1 to single pipe failures shows that 9 pipes have a supply failure magnitude of more than 6% (based on PDA). These pipes with the same ranking are among the top 9 pipes identified by HGA and are illustrated in Fig. 14. In the optimally designed WDN1 (Fig. 12), several pipes have larger diameters or more water flow than the 7th pipe in Fig. 14. However, HGA distinguishes between them and recognizes the critical pipe, as the alternative paths' capacity under the failures is considered in this approach. Moreover, the proposed HGA identifies top pipes with a robustness failure magnitude of more than 5% for this network. There is only a minor difference in the ranking related to the 7th and 8th pipes (Table. A2).

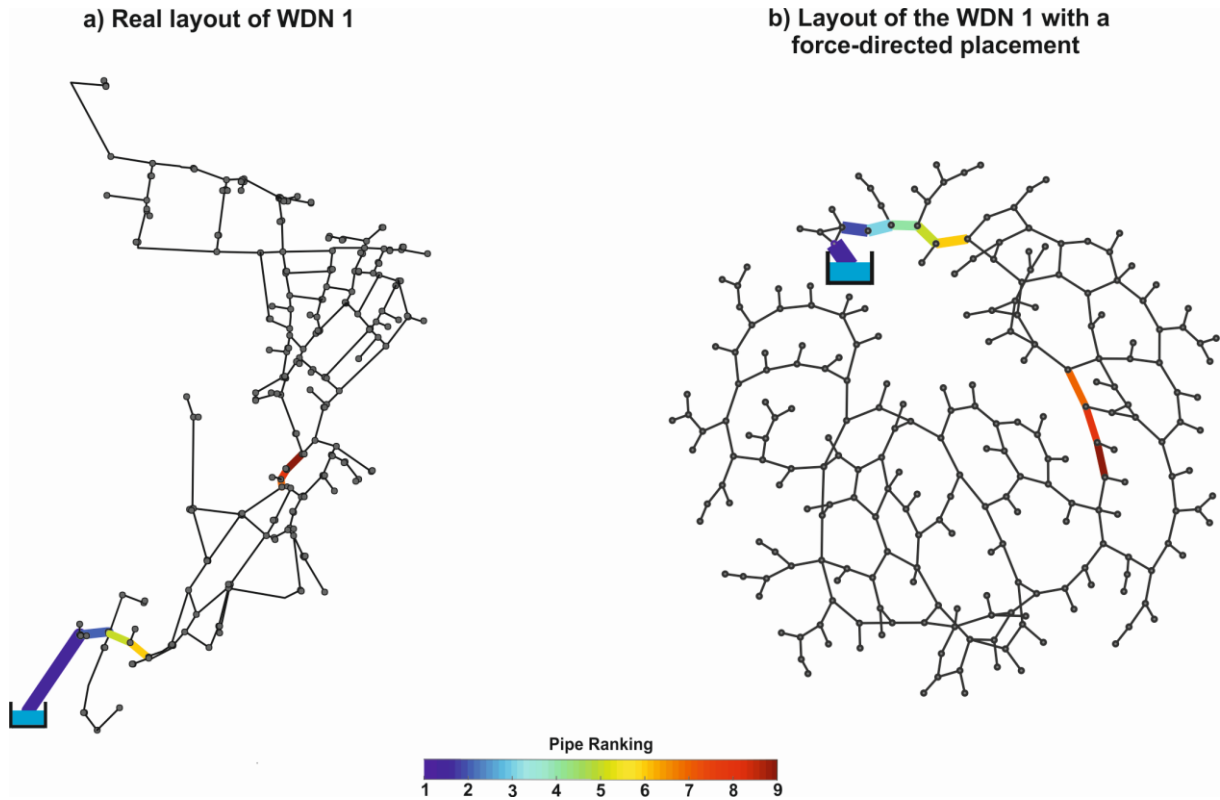


Fig. 14. Critical pipes for the optimally designed WDN 1 with the supply failure magnitudes of more than 6% under single pipe failures

Analyzing the results for the optimally designed WDN 2 showed that the top 13 pipes identified by the graph-based model (i.e., HGA) are all ranked in the top 13 pipes of the PDA model as well (with the same order). For this network, we assess all the pipes whose failure affects the networks (for detailed information see Table. A3). Fig. 15 shows the comparison of the critical pipes derived based on the hydraulic model (a) with those obtained from HGA (b). The thickness of the edges in this figure represents the criticality of the pipes. The results demonstrate that 96% of the pipes with a supply failure magnitude greater than or equal to 1% (44 out of 46) are identified by HGA. The neglected pipes by HGA (i.e., pipes P495 and P454 in Fig 15a) have a low supply failure magnitude (1%) according to the PDA approach.

Besides, the graph-based approach identifies 95% of the pipes with a robustness failure magnitude of more than 1%. Therefore, the proposed HGA can provide remarkably promising results for the resilience analysis of this case study.

The resilience analysis for the optimally designed WDN 3 with two sources shows that 30 pipes have a supply failure magnitude $\geq 1\%$ if they fail individually. As shown in Fig. 16, the HGA can identify all of these pipes with some minor differences in their ranking compared to the hydraulic model. The second source in this network (S2) adds an extra capacity to the system, so the pipe rankings are changed compared to the single-source WDNs. As shown in Fig. 16, the main pipes connecting to the first source are not as critical as they were for the investigated single-source WDNs. The reason is that if S1 is isolated from the network (due to single pipe failure), the provided extra capacity through the pipes connecting to S2 can supply the WDNs. In contrast, in the case of main pipe failures close to S2, the extra capacity between S1 and the nodes is insufficient to support S2. This issue cannot be addressed by the conventional graph measures in the literature. For instance, the LGTM approach (Eq. 17) gives the main pipes connecting to each

source the same ranking, not representing comparable results with the hydraulic model. However, the suggested HGA in this study can properly address the issue by conducting the source tracing and considering the effects of overloaded edges on the resilience of WDNs. In addition, using HGA for the resilience assessment of this network is 3 times faster than the hydraulic simulations in terms of computation efforts. Pipe ranking for this WDN based on HGA takes 46 s, while resilience analysis based on the hydraulic simulations (PDA approach) requires 140 s on a desktop computer (Intel® Core™ i7-8,700 CPU @ 3.2 GHz).

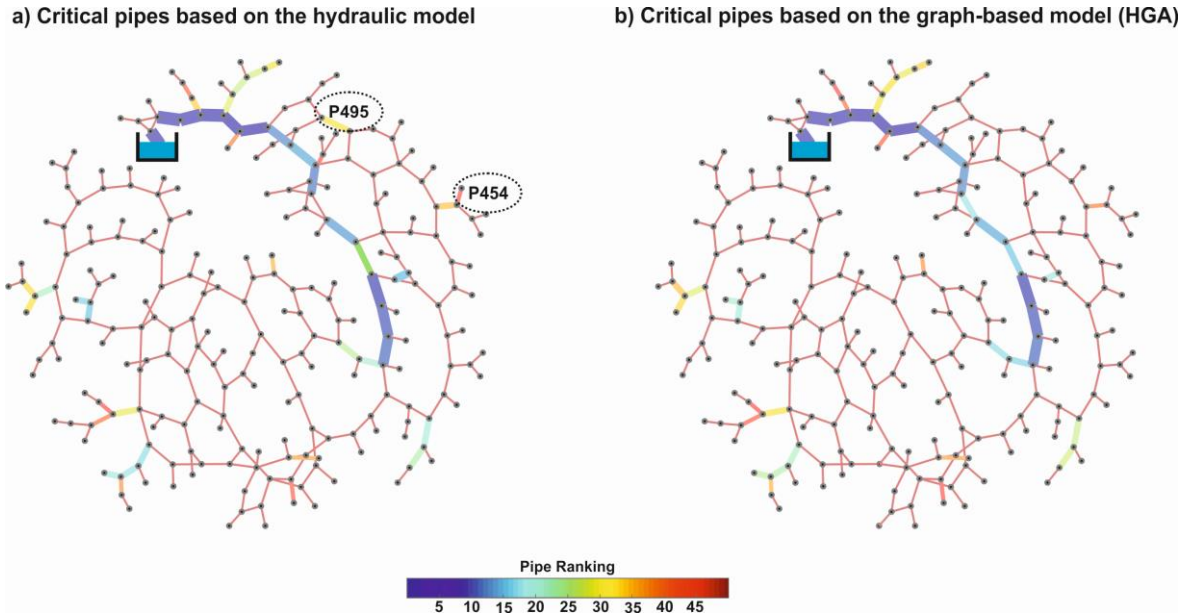


Fig. 15. Critical pipes for optimally designed WDN 2: a) Based on the hydraulic model (PDA) with the supply failure magnitudes $\geq 1\%$, b) Based on HGA

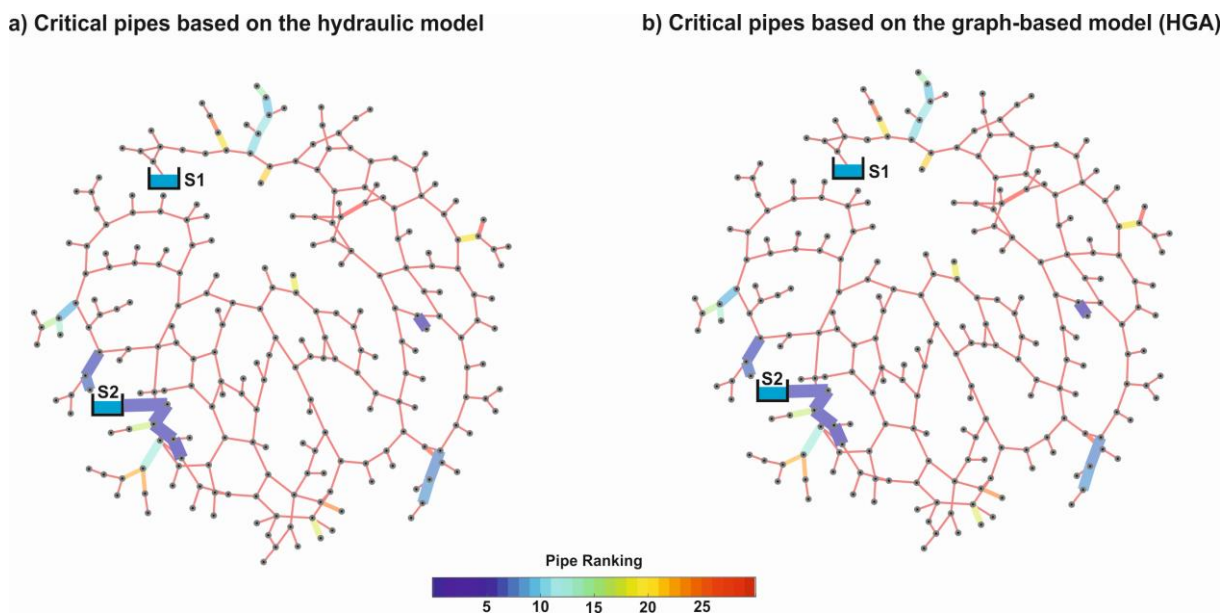


Fig. 16. Critical pipes for optimally designed WDN 3: a) Based on the hydraulic model with the supply failure magnitudes $\geq 1\%$, b) Based on HGA

The results provided in this section reveal another drawback of the conventional graph metrics such as average node degree (Eq. 12), and meshedness coefficient (Eq. 13). The three optimally

designed WDNs evaluated in this section have the same properties as the existing WDN in Table 2. This shows that using topological metrics (like in literature), the resilience measures would be the same for all three design configurations. While using HGA for their resilience assessment can properly differentiate between the results.

4.2 Single pipe failures for the second case study

The response of D-Town to single pipe failure is analyzed using hydraulic simulations and calculating supply failure magnitude. The results are then compared with those obtained from our proposed approach (HGA) and the LGTM method suggested by Pagano et al. (2019) (Eq. 17 and 18). D-Town is comprised of five communities with five demand patterns. This network has a complex hydraulic behavior with seven tanks and five pumping stations (with different operation times). Depending on the operation cycle of the tanks (i.e., emptying/filling), the tanks can play a hydraulic role either as a source node (during the emptying process) or a demand node (during the filling process). The hydraulic role of the tanks in different time steps cannot be recognized by the HGA. However, the network configuration (see Fig. 11b) reveals that the first tank (i.e., T1) acts as an interface between the reservoir and other tanks. This means water needs to transfer from the reservoir to the first tank (T1), and then from T1 to other tanks during the filling process. Therefore, T1 can be considered as the second hub in the system after the reservoir.

Pipe failures could occur during the filling or emptying process of the tanks. Hence, in the HGA procedure, we assume that the failure consequence of a pipe whose removal changes the connections between the reservoir and nodes is the average of impacts during the filling and emptying of T1. This means, for the failure of this pipe, one simulation is conducted when the reservoir is the main source and T1 is filling, and another simulation is performed the other way round. Besides, to mimic the pumps' performance in the graph of WDN, small weights are assigned to pumps, which allows the demand parcel to route through them frequently.

Fig. 17 shows the top 10% of high-ranked pipes (i.e., 40 pipes) according to the hydraulic simulations. 98 % of these pipes (39 out of 40) are among the top 10% of HGA rankings (see Table A4). The only neglected pipe by HGA (P319) is the 40th critical pipe regarding the hydraulic model. This pipe is connected to the pumping station (see Fig.17a), and due to the complex hydraulic of the system, HGA could not recognize it as the critical pipe. However, HGA provides promising results regarding the order of pipe rankings. Only for five pipes of P99, P297, P20, P291, and P996, the difference between the order of rankings derived from HGA and hydraulic simulation is more than five. These pipes are highlighted in Fig. 17a and Table 4A.

To analyze the correlation between the graph method (i.e., HGA) and the hydraulic simulation, Spearman's rank correlation coefficient (Spearman 1904) is calculated. This coefficient evaluates the dependency between the ranking of two variables using a monotonic function (Bolboaca and Jäntschi 2006). The index is between -1 to +1, which shows a perfect positive and negative association of ranks, respectively. In addition, when the value is 0, there is no association of ranks. The Spearman correlation index between the ranking obtained from HGA and the one corresponding to the hydraulic simulations is 0.92, confirming a very strong correlation between them.

On the other hand, the LGTM method creates two subsets of pipes for the pipe rankings, in which most of the order of rankings cannot be compared with those obtained from the hydraulic

simulations (see Table A4). The reason is that the proposed graph measures in the LGTM method only rely on the topological features and cannot capture the real hydraulic behavior of the WDN.

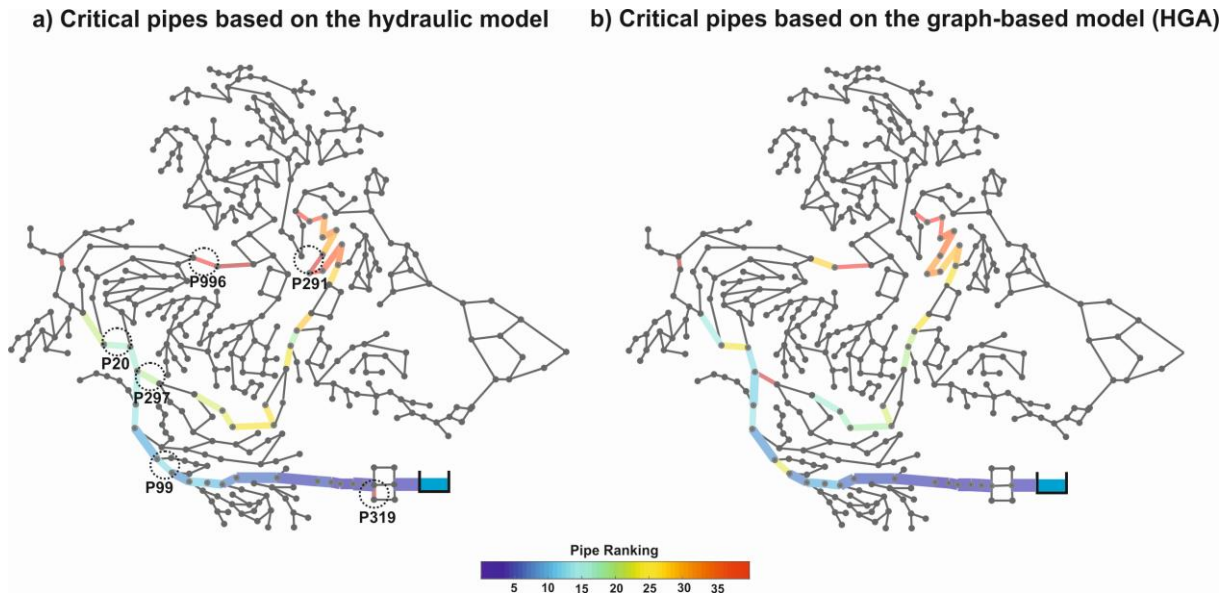


Fig. 17. Top 10% of high-ranked pipes for D-Town: a) Based on the hydraulic model and supply failure magnitudes, b) Based on HGA

4.3 Multiple pipe failures for the third case study

The effect of multiple pipe failures on the resilience of the WDN is assessed in this section. For this purpose, earthquake scenarios are created based on the method described in 2.1.2, and the supply failure magnitude of each scenario is calculated using the hydraulic model. In addition, a convergence study is required to identify an adequate number of Monte Carlo simulations.

According to Fig. 18, the convergence study indicates that 3,000 Monte Carlo simulations are adequate for this network. The values of the supply failure magnitude in this figure are the average values in each Monte Carlo run. In the next step, these 3,000 earthquake scenarios are used as an input for HGA. Therefore, the failure matrix of HGA consists of $58 \times 3,000$ elements, where 58 is the number of edges, and 3,000 is the number of failure scenarios. The effects of each scenario on the network are estimated based on Eq.27 (where $n=s$), and then pipes with the higher values of GI (graph index) are ranked accordingly.

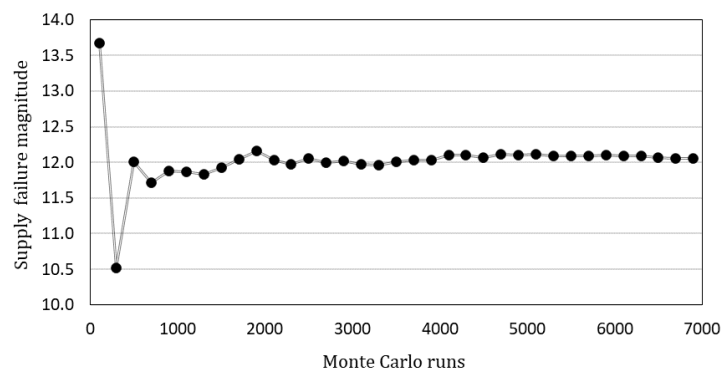


Fig. 18. Convergence study to identify an adequate number of Monte Carlo simulations for BAK WDN

Fig. 19 shows the distribution of the supply failure magnitude of the scenarios (ordered from the maximum value) compared to the corresponding distribution obtained by HGA. GI in this figure is the graph index (Eq. 27) calculated based on the proposed HGA. The x-axis (in Figure 19, right) is set to the logarithmic scale to highlight the comparison between the critical scenarios better. The results show that GI has a similar trend with the values derived from the hydraulic simulations. In addition, most critical scenarios (with the supply failure of more than 20%) are identified by HGA. The Spearman correlation index between hydraulic and graph-based metrics is 0.91, confirming a robust correlation between them. This infers that HGA can represent practical results for identifying critical earthquake scenarios.

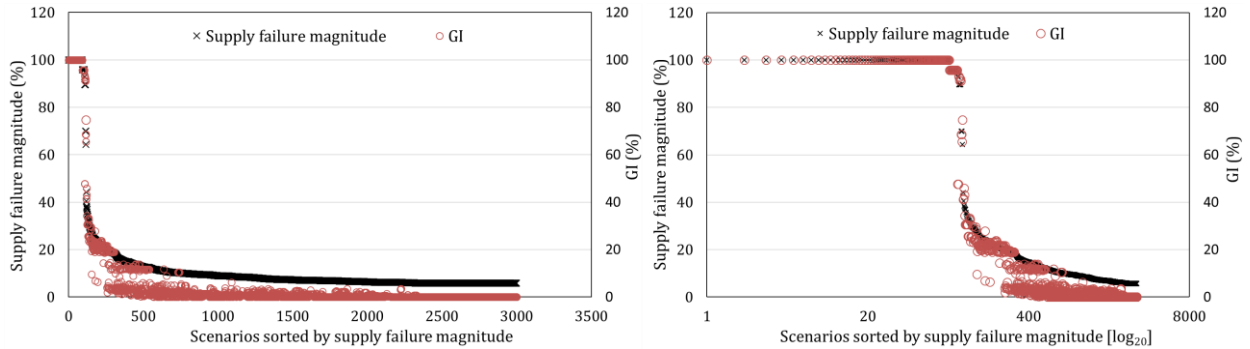


Fig. 19. Comparison between the hydraulic simulations (supply failure) and HGA (GI) for ranking the earthquake scenarios.

5. Next steps

In this report, we indicated the suitability of HGA for ranking the critical pipes of different WDNs under single pipe failures. HGA provided comparable results with the hydraulic model and can be used for critical pipes assessment of networks without hydraulic simulations. The suggested approach also requires less information and computational efforts compared to conventional hydraulic models. In addition, this method was successfully applied to the BAK network with multiple pipe failures (due to earthquakes) to rank the critical scenarios. In the next step, this paper will be extended by proposing a graph-based approach for the resilience enhancement of WDNs in case of multiple pipe failures.

As shown in Fig. 19, HGA could rank the important scenarios based on their GI . After ranking the critical scenarios, the failure matrix F enables us to recognize the most impacted pipes of critical scenarios. In the future, we will select those pipes and redesign them based on a graph-based design approach, which is faster than evolutionary optimization. The results of this method will then be compared with a simulated annealing-based optimization approach which is integrated with a network-level seismic assessment model. Additionally, a comprehensive literature review on seismic rehabilitation of WDNs will be added to this study.

Acknowledgments

I would like to thank Sina Hesarkazzazi, Azadeh Yousefi, and Abhijit Roy for their support and help throughout conducting this report.

The project is part of Mr. Hjaibabaei's Ph.D. program which is funded by the Austrian Science Fund (FWF): P 31104-N29.

6. Appendix

Table A1: Comparing pipe rankings obtained from the hydraulic simulations and HGA for existing network

<i>N</i>	Supply failure magnitude				HGA ranking	Robustness failure magnitude	
	<i>PDA</i>		<i>DDA</i>		<i>Pipe ID</i>	<i>Pipe ID</i>	<i>index</i>
	<i>Pipe ID</i>	<i>index</i>	<i>Pipe ID</i>	<i>index</i>			
1	232	1.00	232	1.00	'232'	232	1.00
2	504	0.98	504	0.98	'504'	504	0.98
3	501	0.98	501	0.98	'501'	501	0.97
4	235	0.97	235	0.97	'235'	235	0.95
5	254	0.95	254	0.95	'254'	254	0.92
6	516	0.94	516	0.94	'516'	516	0.91

Table A2: Comparing pipe rankings obtained from the hydraulic simulations and HGA for the optimally designed network 1

<i>N</i>	Supply failure magnitude				HGA ranking	Robustness failure magnitude	
	<i>PDA</i>		<i>DDA</i>		<i>Pipe ID</i>	<i>Pipe ID</i>	<i>index</i>
	<i>Pipe ID</i>	<i>index</i>	<i>Pipe ID</i>	<i>index</i>			
1	232	1.00	232	1.00	'232'	232	1.00
2	501	0.98	504	0.98	'501'	504	0.98
3	504	0.98	501	0.98	'504'	501	0.97
4	235	0.97	235	0.97	'235'	235	0.95
5	254	0.95	254	0.95	'254'	254	0.92
6	516	0.94	516	0.94	'516'	516	0.92
7	178	0.09	607	0.21	'178'	607	0.08
8	607	0.08	178	0.20	'607'	178	0.07
9	592	0.07	592	0.19	'592'	592	0.06

Table A3: Comparing pipe rankings obtained from the hydraulic simulations and HGA for the optimally designed network 2

N	Supply failure magnitude				HGA ranking	Robustness failure magnitude	
	PDA		DDA		Pipe ID	Pipe ID	index
	Pipe ID	index	Pipe ID	index			
1	232	1.00	232	1.00	'232'	232	1.00
2	504	0.98	504	0.98	'504'	504	0.98
3	501	0.98	501	0.98	'501'	501	0.98
4	235	0.97	235	0.97	'235'	235	0.97
5	254	0.95	254	0.95	'254'	254	0.95
6	516	0.94	516	0.94	'516'	516	0.94
7	607	0.12	607	0.36	'607'	607	0.24
8	178	0.12	178	0.34	'178'	178	0.24
9	592	0.12	592	0.33	'592'	592	0.23
10	225	0.10	225	0.27	'225'	225	0.21
11	529	0.09	474	0.20	'529'	474	0.18
12	474	0.09	529	0.16	'474'	529	0.16
13	484	0.08	484	0.13	'484'	484	0.14
14	601	0.06	601	0.06	'512'	601	0.07
15	40	0.06	40	0.06	'473'	314	0.05
16	314	0.06	314	0.06	'593'	40	0.05
17	347	0.05	347	0.05	'133'	347	0.05
18	349	0.05	349	0.05	'475'	593	0.05
19	574	0.04	574	0.04	'601'	349	0.05
20	441	0.03	593	0.03	'40'	133	0.04
21	593	0.03	441	0.03	'314'	574	0.04
22	317	0.03	133	0.03	'347'	473	0.03
23	195	0.03	195	0.03	'349'	495	0.03
24	133	0.02	317	0.03	'574'	441	0.03
25	525	0.02	528	0.02	'441'	195	0.03
26	528	0.02	523	0.02	'195'	317	0.03
27	523	0.02	525	0.02	'317'	475	0.02
28	342	0.02	342	0.02	'528'	523	0.02
29	260	0.01	35	0.01	'523'	525	0.02
30	35	0.01	260	0.01	'525'	528	0.02
31	495	0.01	558	0.01	'342'	342	0.02
32	558	0.01	509	0.01	'35'	260	0.01
33	509	0.01	570	0.01	'260'	35	0.01
34	458	0.01	581	0.01	'558'	558	0.01
35	396	0.01	396	0.01	'570'	509	0.01
36	581	0.01	458	0.01	'581'	458	0.01
37	570	0.01	521	0.01	'396'	396	0.01

38	521	0.01	345	0.01	'458'	581	0.01
39	345	0.01	344	0.01	'509'	570	0.01
40	510	0.01	427	0.01	'521'	521	0.01
41	427	0.01	510	0.01	'345'	510	0.01
42	344	0.01	439	0.01	'344'	467	0.01
43	482	0.01	482	0.01	'427'	427	0.01
44	454	0.01	454	0.01	'510'	345	0.01
45	439	0.01			'439'		
46	473	0.01			'482'		

Table A4. Comparing pipe rankings obtained from the hydraulic simulations, HGA and LTTM for D-Town

Pipe ID	Hydraulic model ranking (based on supply failure magnitude)	HGA ranking (This study)	LGTM ranking (Pagano et al. 2019)	
			Based on Eq. 17	Based on Eq. 18
P310	Rank 1	Rank 1	Rank 18	
P316	Rank 2	Rank 2	Rank 19	
P98	Rank 3	Rank 3	Rank 17	
P83	Rank 4	Rank 5	Rank 15	
P97	Rank 5	Rank 4	Rank 16	
P22	Rank 6	Rank 7	Rank 13	
P100	Rank 7	Rank 6	Rank 14	
P23	Rank 8	Rank 8	Rank 12	
P25	Rank 9	Rank 9	Rank 10	
P34	Rank 10	Rank 10	Rank 9	
P102	Rank 11	Rank 11	Rank 8	
P24	Rank 12	Rank 13		Rank 26
P110	Rank 13	Rank 12		Rank 24
P99	Rank 14	Rank 24		Rank 19
P17	Rank 15	Rank 16		Rank 21
P18	Rank 16	Rank 14		Rank 20
P19	Rank 17	Rank 15	Rank 1	

P20	Rank 18	Rank 25	Rank 18	
P468	Rank 19	Rank 22	Rank 11	
P297	Rank 20	Rank 39		Rank 17
P21	Rank 21	Rank 17		Rank 39
P892	Rank 22	Rank 18	Rank 2	
P96	Rank 23	Rank 19	Rank 3	
P467	Rank 24	Rank 21	Rank 5	
P445	Rank 25	Rank 20	Rank 4	
P465	Rank 26	Rank 23		
P237	Rank 27	Rank 26		Rank 2
P379	Rank 28	Rank 27		Rank 1
P308	Rank 29	Rank 33		Rank 7
P256	Rank 30	Rank 35		Rank 9
P252	Rank 31	Rank 34		Rank 8
P238	Rank 32	Rank 30		Rank 3
P292	Rank 33	Rank 29		Rank 4
P933	Rank 34	Rank 36		Rank 10
P934	Rank 35	Rank 37		Rank 11
P293	Rank 36	Rank 32		Rank 5
P996	Rank 37	Rank 28	Rank 6	
P291	Rank 38	Rank 31		Rank 6
P397	Rank 39	Rank 38	Rank 7	
P319	Rank 40	Rank 52		

7. References

- Abrahamson, N. A. and W. J. Silva. 2007. "Campbell-Bozorgnia NGA Ground Motion Relations for the Geometric Mean Horizontal Component of Peak and Spectral Ground Motion Parameters." *Berkeley, CA: Pacific Earthquake Engineering Research Center, Univ. of California*.
- Adachi, Takao. 2007. "Impact of Cascading Failures on Performance Assessment of Civil Infrastructure Systems."
- ALA. 2001. "Seismic Fragility Formulations for Water Systems." *Washington, DC: ALA (American Lifelines Alliance)*.
- Assad, Ahmed, Osama Moselhi, and Tarek Zayed. 2019. "A New Metric for Assessing Resilience of Water Distribution Networks." *Water* 11(8):1701.
- Bolboaca, Sorana-Daniela and Lorentz Jäntschi. 2006. "Pearson versus Spearman, Kendall's Tau Correlation Analysis on Structure-Activity Relationships of Biologic Active Compounds." *Leonardo Journal of Sciences* 5(9):179–200.
- Brandes, Ulrik. 2008. "On Variants of Shortest-Path Betweenness Centrality and Their Generic Computation." *Social Networks* 30(2):136–45.
- Buhl, J., J. Gautrais, N. Reeves, R. V Solé, S. Valverde, P. Kuntz, and G. Theraulaz. 2006. "Topological Patterns in Street Networks of Self-Organized Urban Settlements." *The European Physical Journal B-Condensed Matter and Complex Systems* 49(4):513–22.
- Butler, David, Sarah Ward, Chris Sweetapple, Maryam Astaraiie-Imani, Kegong Diao, Raziye Farmani, and Guangtao Fu. 2017. "Reliable, Resilient and Sustainable Water Management: The Safe & SuRe Approach." *Global Challenges* 1(1):63–77.
- Chen, Thomas Ying-Jeh, Greta Vladeanu, and Craig Michael Daly. 2021. "Pipe Criticality Assessment without a Hydraulic Model." Pp. 115–24 in *Pipelines 2021*.
- Diao, Kegong, Chris Sweetapple, Raziye Farmani, Guangtao Fu, Sarah Ward, and David Butler. 2016. "Global Resilience Analysis of Water Distribution Systems." *Water Research* 106:383–93.
- Dijkstra, Edsger W. 1959. "A Note on Two Problems in Connexion with Graphs." *Numerische Mathematik* 1(1):269–71.
- Field, Edward H., Hope A. Seligson, Nitin Gupta, Vipin Gupta, Thomas H. Jordan, and Kenneth W. Campbell. 2005. "Loss Estimates for a Puente Hills Blind-Thrust Earthquake in Los Angeles, California." *Earthquake Spectra* 21(2):329–38.
- Giudicianni, C., M. Herrera, A. Di Nardo, R. Greco, E. Creaco, and A. Scala. 2020. "Topological Placement of Quality Sensors in Water-Distribution Networks without the Recourse to Hydraulic Modeling." *Journal of Water Resources Planning and Management* 146(6):4020030.
- Giustolisi, Orazio, Luca Ridolfi, and Antonietta Simone. 2019. "Tailoring Centrality Metrics for Water Distribution Networks." *Water Resources Research* 55(3):2348–69.
- Gorev, Nikolai B., Vyacheslav N. Gorev, Inna F. Kodzheshirova, Igor A. Shedlovsky, and P. Sivakumar. 2021. "Technique for the Pressure-Driven Analysis of Water Distribution Networks with Flow- and Pressure-Regulating Valves." *Journal of Water Resources Planning and Management* 147(5):06021005.
- Hajibabaei, Mohsen, Sina Hesarkazzazi, and Robert Sitzenfrei. 2021. "Optimization of Water

- Distribution Networks with Dynamic Edge Betweenness Centrality – A Sensitivity Analysis.” in *World Environmental and Water Resources Congress 2021*.
- Hajibabaei, Mohsen, Sara Nazif, and Robert Sitzenfrei. 2019. “Improving the Performance of Water Distribution Networks Based on the Value Index in the System Dynamics Framework.” 1–23.
- Herrera, Manuel, Edo Abraham, and Ivan Stoianov. 2016. “A Graph-Theoretic Framework for Assessing the Resilience of Sectorised Water Distribution Networks.” *Water Resources Management* 30(5):1685–99.
- Hwang, Hwee and Kevin Lansey. 2017. “Water Distribution System Classification Using System Characteristics and Graph-Theory Metrics.” *Journal of Water Resources Planning and Management* 143(12):4017071.
- Jayaram, Nirmal and Jack W. Baker. 2009. “Correlation Model for Spatially Distributed Ground-motion Intensities.” *Earthquake Engineering & Structural Dynamics* 38(15):1687–1708.
- Jung, Donghwi, Seungyub Lee, and Joong Hoon Kim. 2019. “Robustness and Water Distribution System: State-of-the-Art Review.” *Water* 11(5):974.
- Lorenz, Imke-Sophie, Lena C. Altherr, and Peter F. Pelz. 2021. “Resilience Enhancement of Critical Infrastructure–Graph-Theoretical Resilience Analysis of the Water Distribution System in the German City of Darmstadt.” Pp. 137–49 in *World Congress on Engineering Asset Management*. Springer.
- Lorenz, Imke-Sophie and Peter F. Pelz. 2020. “Optimal Resilience Enhancement of Water Distribution Systems.” *Water* 12(9):2602.
- Mahmoud, Herman A., Dragan Savić, and Zoran Kapelan. 2017. “New Pressure-Driven Approach for Modeling Water Distribution Networks.” *Journal of Water Resources Planning and Management* 143(8):04017031.
- Meng, Fanlin, Guangtao Fu, Raziye Farmani, Chris Sweetapple, and David Butler. 2018. “Topological Attributes of Network Resilience: A Study in Water Distribution Systems.” *Water Research* 143:376–86.
- Newman, Mark. 2010. *Networks: An Introduction*. New York. Oxford, UK: Oxford University Press.
- ÖNORM, B. 2018. “2538 Long-Distance, District and Supply Pipelines of Water Supply Systems–Additional Specifications Concerning ÖNORM EN 805.” *Österreichisches Normungsinstitut, Vienna, Austria*.
- Pagano, Alessandro, Chris Sweetapple, Raziye Farmani, Raffaele Giordano, and David Butler. 2019. “Water Distribution Networks Resilience Analysis: A Comparison between Graph Theory-Based Approaches and Global Resilience Analysis.” *Water Resources Management* 33(8):2925–40.
- Pandit, Arka and John C. Crittenden. 2016. “Index of Network Resilience for Urban Water Distribution Systems.” *International Journal of Critical Infrastructures* 12(1–2):120–42.
- Perelman, Lina Sela, Michael Allen, Ami Preis, Mudasser Iqbal, and Andrew J. Whittle. 2015. “Flexible Reconfiguration of Existing Urban Water Infrastructure Systems.” *Environmental Science & Technology* 49(22):13378–84.
- Rossman, L., H. Woo, M. Tryby, F. Shang, R. Junke, and T. Haxton. 2020. “Epanet 2.2 User Manual.” *Cincinnati: EPA*.
- Shuang, Qing, Mingyuan Zhang, and Yongbo Yuan. 2014. “Node Vulnerability of Water Distribution Networks under Cascading Failures.” *Reliability Engineering & System Safety*

124:132–41.

- Simone, Antonietta, Francesco G. Ciliberti, Daniele B. Laucelli, Luigi Berardi, and Orazio Giustolisi. 2020. "Edge Betweenness for Water Distribution Networks Domain Analysis." *Journal of Hydroinformatics* 22(1):121–31.
- Sitzenfrei, Robert. 2021. "Using Complex Network Analysis for Water Quality Assessment in Large Water Distribution Systems." *Water Research* 117359.
- Sitzenfrei, Robert, Martin Oberascher, and Jonatan Zischg. 2019. "Identification of Network Patterns in Optimal Water Distribution Systems Based on Complex Network Analysis." Pp. 473–83 in *World Environmental and Water Resources Congress 2019: Hydraulics, Waterways, and Water Distribution Systems Analysis*. American Society of Civil Engineers Reston, VA.
- Sitzenfrei, Robert, Qi Wang, Zoran Kapelan, and Dragan Savić. 2020. "Using Complex Network Analysis for Optimization of Water Distribution Networks." *Water Resources Research* 56(8):e2020WR027929.
- Sitzenfrei, Robert, Qi Wang, Zoran Kapelan, and Dragan Savić. 2021. "A Complex Network Approach for Pareto-Optimal Design of Water Distribution Networks." Pp. 901–13 in *World Environmental and Water Resources Congress*.
- Spearman, C. 1904. "The Proof and Measurement of Association Between Two Things, *American J.*"
- Strigini, Lorenzo. 2012. "Fault Tolerance and Resilience: Meanings, Measures and Assessment." Pp. 3–24 in *Resilience assessment and evaluation of computing systems*. Springer.
- Tabesh, M. and A. Zia. 2003. "Dynamic Management of Water Distribution Networks Based on Hydraulic Performance Analysis of the System." *Water Science and Technology: Water Supply* 3(1–2):95–102.
- Tanyimboh, Tiku T. and Andrew B. Templeman. 2010. "Seamless Pressure-Deficient Water Distribution System Model." Pp. 389–96 in *Proceedings of the institution of civil engineers-water management*. Vol. 163. Thomas Telford Ltd.
- Torres, Jacob M., Leonardo Duenas-Osorio, Qilin Li, and Alireza Yazdani. 2017. "Exploring Topological Effects on Water Distribution System Performance Using Graph Theory and Statistical Models." *Journal of Water Resources Planning and Management* 143(1):4016068.
- Ulusoy, Aly Joy, Ivan Stoianov, and Aurelie Chazerain. 2018. "Hydraulically Informed Graph Theoretic Measure of Link Criticality for the Resilience Analysis of Water Distribution Networks." *Applied Network Science* 3(1).
- USGS. 2018. "U.S. Quaternary Faults and Folds Database."
- Wagner, Janet M., Uri Shamir, and David H. Marks. 1988. "Water Distribution Reliability: Simulation Methods." *Journal of Water Resources Planning and Management* 114(3):276–94.
- Wang, Min and Tsuyoshi Takada. 2005. "Macrosatial Correlation Model of Seismic Ground Motions." *Earthquake Spectra* 21(4):1137–56.
- Wang, Q., D. A. Savić, and Z. Kapelan. 2017. "GALAXY: A New Hybrid MOEA for the Optimal Design of Water Distribution Systems." *Water Resources Research* 53(3):1997–2015.
- Weatherill, G., V. Silva, H. Crowley, and P. Bazzurro. 2013. "Exploring Strategies for Portfolio Analysis in Probabilistic Seismic Loss Estimation." in *Proceedings of Vienna Congress on Recent Advances in Earthquake Engineering and Structural Dynamics*.

- Yazdani, A., R. Appiah Otoo, and Paul Jeffrey. 2011. "Resilience Enhancing Expansion Strategies for Water Distribution Systems: A Network Theory Approach." *Environmental Modelling & Software* 26(12):1574–82.
- Yazdani, Alireza, Leonardo Dueñas-Osorio, and Qilin Li. 2013. "A Scoring Mechanism for the Rank Aggregation of Network Robustness." *Communications in Nonlinear Science and Numerical Simulation* 18(10):2722–32.
- Zanini, M. A., C. Vianello, F. Faleschini, L. Hofer, and G. Maschio. 2016. "A Framework for Probabilistic Seismic Risk Assessment of NG Distribution Networks." *Chemical Engineering Transactions* 53:163–68.
- Zanini, Mariano Angelo, Flora Faleschini, and Carlo Pellegrino. 2017. "Probabilistic Seismic Risk Forecasting of Aging Bridge Networks." *Engineering Structures* 136:219–32.
- Zhang, Mingyuan, Juan Zhang, Gang Li, and Yuan Zhao. 2020. "A Framework for Identifying the Critical Region in Water Distribution Network for Reinforcement Strategy from Preparation Resilience." *Sustainability (Switzerland)* 12(21):1–17.
- Zhao, Xudong, Zhilong Chen, and Huadong Gong. 2015. "Effects Comparison of Different Resilience Enhancing Strategies for Municipal Water Distribution Network: A Multidimensional Approach." *Mathematical Problems in Engineering* 2015.